Experimental study of the mechanical behaviour of a new extruded earth block masonry

Elsevier Editorial System(tm) for
Construction & Building Materials
Manuscript Draft

Manuscript Number: CONBUILDMAT-D-19-08914R1

Title: Experimental study of the mechanical behaviour of a new extruded earth block masonry

Article Type: Research Paper

Keywords: earth masonry; digital image correlation; shear behaviour; diagonal compression; failure mechanism; compressive behaviour; full-field strain.

Corresponding Author: Professor Francesca Stazi, Associate Professor

Corresponding Author's Institution: Università Politecnica delle Marche

First Author: Francesca Stazi, Associate Professor

Order of Authors: Francesca Stazi, Associate Professor; Michele Serpilli, Assistant Professor; Gianluca Chiappini, Ph.D, Researcher; Marianna Pergolini, Ph.D; Evelina Fratalocchi, Associate Professor; Stefano Lenci, Full Professor

Abstract: The aim of this research is to investigate, through the Digital Image Correlation (DIC) technique, the mechanical performance of a new type of earth masonry, built with extruded blocks and characterized by dovetail horizontally staggered bed joints. The experimental program consists of two levels of investigations: (i) preliminary phase on components, (ii) compression, diagonal compression and combined shear-compression tests on 12 wallettes. Regarding the components, results showed that the mean compressive strength of the earth block was low (3.5 MPa) with respect to traditional bricks and similar to adobe blocks. The dovetail joints were effective in their joining role showing a rather good strength (2.4 MPa) when tested in triplet configuration. Regarding the wallettes, the DIC highlighted failure modes complying with the ones of a traditional masonry under shear, while it showed a "column behaviour" with vertical sliding under compressive tests. Fragile failures occurred during the diagonal compression test. DIC revealed to be a promising technique to recover the full-field strain and crack maps

Cover letter

February 3rd, 2020

Department of Materials, Environmental Sciences and Urban Planning (SIMAU)
Università Politecnica delle Marche, Via Brecce Bianche, 60131, Ancona, Italy.

Dear Editorial Board of Construction and Building Materials,

I am writing to submit the revised version of our manuscript entitled “Experimental study of the mechanical behaviour of a new extruded earth block masonry”.

The revision allowed us improving the manuscript: some concepts were clarified, more details on block materials and type of extrusion were added, the images were corrected as specified by the reviewers and new references were introduced in the discussion section.

As regards the obtained results, the Digital Image Correlation (DIC) showed its potential in the stress-strain monitoring framework, allowing a complete reconstruction of the strains fields of the masonry wallettes. The technique highlighted failure modes complying with the ones of a traditional masonry under shear while showed a “column behaviour” with vertical sliding under compressive tests.

These contents are original. Each of the authors confirms that this manuscript has not been previously published and is not currently under consideration by any other journal. Additionally, all authors have seen and approved this revised version of the paper and have agreed to the Journal‘s submission policies.

Thank you and best regards,

Francesca Stazi
Corresponding Author
Università Politecnica delle Marche Via Brecce Bianche, 60131, Ancona, Italy.
E-mail: f.stazi@univpm.it

Experimental study of the mechanical behaviour of a new extruded earth block masonry

Francesca Stazi[(a)]

Corresponding author

f.stazi@univpm.it

Michele Serpilli[(b)]

m.serpilli@univpm.it

Gianluca Chiappini[(c)]

g.chiappini@univpm.it

Marianna Pergolini[(a)]

m.pergolini@hotmail.it

Evelina Fratalocchi [(a)]

e.fratalocchi@univpm.it

Stefano Lenci [(b)]

s.lenci@univpm.it

(a) Department of Materials, Environmental Sciences and Urban Planning (SIMAU), Università Politcnica delle Marche, Italy.

(b) Department of Construction, Civil Engineering and Architecture (DICEA) Università Politcnica delle Marche, Italy.

(c) Department of Industrial Engineering and Mathematical Sciences (DIISM) Università Politcnica delle Marche, Italy.

Experimental study of the mechanical behaviour of a new extruded earth block masonry

F. Stazi[(a)], M. Serpilli[(b)], G. Chiappini[(c)], M. Pergolini[(a)], E. Fratalocchi[(a)], S. Lenci[(b)]

(a) Department of Materials, Environmental Sciences and Urban Planning (SIMAU), Università Politecnica delle Marche, Italy.

(b) Department of Civil and Construction Engineering, and Architecture (DICEA) Università Politecnica delle Marche, Italy.

(c) Department of Industrial Engineering and Mathematical Sciences (DIISM) Università Politecnica delle Marche, Italy.

Keywords: earth masonry; digital image correlation; shear behaviour; diagonal compression; failure mechanism; compressive behaviour; full-field strain.

ABSTRACT

The aim of this research is to investigate, through the Digital Image Correlation (DIC) technique, the mechanical performance of a new type of earth masonry, built with extruded blocks and characterized by dovetail horizontally staggered bed joints. The experimental program consists of two levels of investigations: (i) preliminary phase on components, (ii) compression, diagonal compression and combined shear-compression tests on 12 wallettes. Regarding the components, results showed that the mean compressive strength of the earth block was low (3.5 MPa) with respect to traditional bricks and similar to adobe blocks. The dovetail joints were effective in their joining role showing a rather good strength (2.4 MPa) when tested in triplet configuration. Regarding the wallettes, the DIC highlighted failure modes complying with the ones of a traditional masonry under shear, while it showed a "column behaviour" with vertical sliding under compressive tests. Fragile failures occurred during the diagonal compression test. DIC revealed to be a promising technique to recover the full-field strain and crack maps.

Nomenclature

f_c compressive strength of the earth block

f_{cm} average compressive strength of the earth block

f_{voi} initial shear strength

f_{vo} average initial shear strength

f_{vok} characteristic initial shear strength

E_i Young modulus

ν Poisson ratio

τ shear stress

σ normal stress

τ_m wall average shear strength

σ_m wall average compressive strength

G shear modulus

γ shear strain

ε normal strain

s_x horizontal displacement

s_y vertical displacement

1. Introduction

The present research focuses on a new type of masonry made of earth blocks. Benefits associated with the adoption of earth units include the improvement of the building energy efficiency [1, 2], and its environmental and economic sustainability [3-5]. The blocks are made of a mixture of natural components, namely clay, water and rice husk fibres. Clay acts as a natural binder and confers strength to the blocks but it can be subject to cracks due to drying shrinkage [6]. This drawback can be reduced through the addition of stabilizers. Numerous studies suggest the use of both natural [7-9] and artificial [10] fibres to prevent the outbreak of tensile forces and the consequent drying shrinkage [11]. Another relevant feature affecting the performance of earth blocks is represented by the manufacturing process that can vary from manual to fully automated [12-14]. The extrusion of bricks is a promising method, determining strengths comparable with those of traditional fired bricks [15].

While there is a lot of literature on mechanical behavior of stone and fired brick masonries, the knowledge on extruded earth blocks constructions is very limited. Indeed the literature on earthen wallettes mainly regards the most commonly used earth construction techniques, namely rammed earth [12, 14, 16 and 17] and cob [12], while the studies on extruded earth block masonries are very rare. The earth blocks adopted in [12] and [13] are brick-like units produced by a mechanized hand-moulding procedure, horizontally layered with mortar bed joints, thus recreating a traditional masonry wall.

In this research, we have selected extruded perforated blocks with rice husk, to couple a natural stabilization method with the most advantageous manufacturing technique (Fig.1a). The block is novel since the extrusion is uncommonly-realized at industrial scale, providing a major structural potential with respect to usual blocks, which are manually or mechanically compressed within a mold. Moreover, a novel assembly technique for the masonry construction is adopted, providing horizontally staggered bed joints (thus creating aligned vertical joints), linked through tongue and groove dovetail connections. This technique is at the present used in both exterior and interior sides of timber framed constructions (Fig.1 b and c), fixed by means of ring-shank nails to the external bracing fir boards, with energy saving and shear-collaborating issues, but without load bearing functions.

In the present work, the new earth block masonry was surveyed through Digital Image Correlation (DIC). In recent years, this technique has become one of the most promising measurement methods, since it allows obtaining a significant amount of information on the strain state of the material/structure and a complete reconstruction of the crack pattern [18]. Several authors have

advantageously applied DIC in different frameworks, such as the analysis of the mechanical behaviour of reinforced concrete beams [19-21], composites [20] and masonry.
Its application on masonries was carried out at different scales: characterization of small specimens of reinforcing mortars [21]; investigation of the bonding behaviour in FRP–brick specimens interfaces [22]; survey of the mechanical behaviour of small-scale masonry units [23]; tests on wallettes and full-scale prototypes ([24] and [25]); mechanical study of real-scale confined masonry walls [26]; map of the crack propagation at the building scale [27].

The present research is aimed at characterizing the mechanical properties of a new type of masonry with horizontally staggered bed joints, made of extruded earth blocks by means of the DIC technique and evaluating possible applications of such blocks for load bearing functions.
To that aim, an extensive experimental campaign has been carried out by means of compression and shear tests on small samples and wallettes. All measurements have been recorded with the aid of DIC technique and processed via MatLab.

2. Test methods

The research phases are the following:

- Preliminary phase: material characterization of earth blocks to obtain the compressive strength of single units and the initial shear strength of triplets.
- Main phase: characterization of the mechanical behavior of earth blocks wallettes through DIC technique to obtain the displacement and strain fields.

A detailed outline of the lab tests of the main phase is summarized in Table 1.

2.1. Materials and samples preparation

The hollow extruded earth blocks were provided by Ton-Gruppe Construction Company.
Their composition consists of a matrix of clayey soil (70%) and spoils of rice husk fibers (30%) as natural stabilizers. The rice husk fibers have size of about 3 mm x 5 mm. The extruded blocks have been mechanically produced with the same manufacturing process used in brick factories, except for the oven and artificial drying chambers.
The soil matrix was tested to determine its grain size distribution (ASTM D422) and consistency limits (ASTM D4318). All the soil passed the #200 sieve (opening 0,075 mm) and resulted a lean clay according to the Unified Soil Classification System, USCS (ASTM D2487), as shown in Table

2 and Fig. 2. The activity coefficient, equal to about 1, reveals a normally active soil, with a low susceptibility to swelling or shrinkage. X-ray diffractometry revealed that the main mineralogical components are calcite, montmorillonite and gypsum as shown in Table 3.

The tested samples consisted of 9 single blocks, 6 triplets and 12 wallettes.

The block is extruded through a die machine and left naturally air-dried. Each earth unit has nominal dimensions of (215 x 230 x 115 mm^3) and presents one flat vertical surface and one ribbed side to improve the adhesion of the external plaster **(**Fig. 1a**)**. On the lateral surfaces, dovetail joints serve as a guide for the alignment of the earth units during the wall assembly and ensure their mechanical connection, thus enhancing the overall global behavior. A novel technique for the wall assembly with horizontally staggered bed joints is adopted. Thus, the blocks are aligned along vertical columns and are linked together through the aforementioned dovetail joints.

The wallets size was 1.07 x 1.03 x 0.11 m^3. Their realization comprised the following steps: (i) clay was mixed with water in a ratio of 2:1; (ii) the lateral and the bottom surfaces of each block were uniformly wetted in this paste; (iii) each block was then secured to the others by vertically sliding it along their dovetail joints.

Preliminary tests on mortar samples (UNI EN 1015-11:2017) revealed values of 0.21 N/mm^2 and 1.83 N/mm^2, respectively for flexural and compression strengths. The upper bed of each specimen was leveled to remove excess material as to guarantee a plane surface for the subsequent load application.

All materials and assemblies were stored in the laboratory until testing and the curing process lasted 30 days in a controlled laboratory environment.

2.2. Preliminary tests on the earth blocks

The net compressive strength of nine uncapped earth blocks (Fig. 3a) was determined in accordance to the UNI EN 772-1:2015 standard. The testing apparatus was a hydraulic press machine (maximum load capacity of 5000 kN). The rate of compression was set at 0.05 ($N/mm^2/s$). The earth blocks were tested in the extrusion direction.

The initial shear strength parallel to the dovetail joints (Fig. 3b) was determined on 3 specimens according to UNI EN 1052-3:2007 standard (Procedure B). The test set up involved the use of two 20-mm thick plates at the top and at the bottom of the specimen. Compressive load was applied on the top plate using of Zwick Roell Z050 testing machine (maximum load of 1000 kN) in force control at a rate of 2645 N/min until failure.

The initial shear strength perpendicular to the dovetail joints (Fig. 3c), subject to an out-of-plane load, was evaluated on 3 specimens by adopting the same UNI EN 1052-3:2007 standard procedure.

2.3. DIC Set-up

The displacement and deformation of the surface of the wallettes were measured using the 3D-DIC technique. The region of interest (ROI) on each side of the wallettes has been spray-painted with black and white texture. Preliminary tests were carried out to define the most suitable dimensions and intensity of the pattern, following [24]. The experimental set-up is presented in Fig. 4. The features of the two cameras (model Pixelink® B371F – see insert A in Fig. 4) and the calibration data are shown in Table 4.

A third camera (insert A in Fig. 4) was used to check, with DIC-2D, the displacement and the deformation of the backside. During the tests, the manometer was coupled with an additional high-resolution camera that acquired the frames needed to register the pressure trend against time. Then, compression and tensile strengths values were obtained, according to the relative test standards.

The pictures of the wallettes acquired during the tests have been post-processed by a 3D-DIC software. The correlation method between the two cameras and the deformed images was based on global DIC, which incorporates the epipolar constraint and the assembling approach of Finite Element method. The displacements of all grid measuring points, created on the entire surface of the wallettes, were obtained by minimizing the correlation error computed all over the current frame with respect to the reference frame [25]. The zero-mean sum of square difference (ZSSD) criterion has been adopted to avoid the effects of lighting offset and inhomogeneity.

Fig. 5a presents one of the pictures recorded by the frontal camera with the overlaid measurement grid. The subsets discretization, used for the DIC analysis, was 25×25 pixels meaning each measure point was about 20 mm. Fig. 5b shows the 3D grid calculated by the stereo triangulation with the schematic position of the two frontal cameras. The strains (γ_x, γ_y, and γ_{xy}) have been computed by means of the Cauchy-Green theory, starting from the 3D node displacements. Several authors have already successfully applied this method on tests of different materials: metals, ceramic, foam, cork and FRCM [28-32].

In a preliminary phase, the quality of the correlation technique and strains measurements was assessed through a set of 50 stationary images. Fig. 5c illustrates the average values of the vertical strain distribution (ε_y) and its standard deviation within each frame. The average strain presents small random oscillations around zero and the standard deviations are nearly constant, in the order

of 100 με. The crack maps were obtained by calculating the equivalent Von Mises strain in plane strain conditions (γ_3=0) [33].

$$\varepsilon_{VM} = \sqrt{\frac{2\left[(\varepsilon_1 - \varepsilon_2)^2 + \varepsilon_1^2 + \varepsilon_2^2\right]}{3}} \quad (1)$$

To avoid visualizing the sliding effect between columns of bricks, the crack maps were calculated by creating measurement grids on each brick column separately.

2.4. Tests on the wallettes

The compressive strength of the wallettes (Fig. 6a) was determined on 3 samples according to UNI EN 1052-1. The specimens were subject to a compression load by means of two 500 kN hydraulic jacks, uniformly distributed thanks to a 25 mm-thick steel plate. The nominal strains ε were obtained by averaging the strain values recorded through DIC on the whole specimen area.

The shear strength of the wallettes (Fig. 6b) was obtained through diagonal compression tests on 3 samples following the ASTM E519 – 07 standards. The shear test apparatus consisted of a single hydraulic jack (500 kN). The shear strain γ was estimated through DIC, as the mean value of the γ recorded on the ROI.

The shear strength of the wallettes under a constant pre-compression load (Fig. 6c) was obtained on 3 samples following the experimental guidelines provided by [34], using a pre-compression load of 0.2 N/mm^2. An "L" shaped steel profile was placed on the upper part of the specimen to transmit the horizontal force.

3. Results of preliminary tests

The compressive strengths of the earth blocks, referred to the net area (the area of the surface on which the load is applied excluding the voids), are summarized in Table 5.

The average net compressive strength f_{cm} was found to be 3.4 N/mm^2. As expected, this value is quite low as compared to the compressive strength of traditional solid baked bricks, commonly around 16 N/mm^2 [35].

The failure mode was the same for all the specimens tested, with cracks originating before the peak load (Fig. 7a). Cracks were located on the front and backsides of the blocks, close to the point of application of the load.

The average and characteristic initial shear strengths f_{voi} and f_{vok} parallel and perpendicular to the dovetail joints are reported in Table 6. The characteristic initial shear strength f_{vok} parallel to the dovetail joints was 0.03 N/mm^2. The coefficient of variation (COV) is relatively high, as typical in handmade assembled constructions. The typical failure mode is reported in Fig. 7b. The characteristic initial shear strength f_{vok} perpendicular to the dovetail joints was 1.90 N/mm^2. The failure mode is reported in Fig. 7c, denoting a good interlocking effect of the dovetail joint and corner expulsion.

4. Normal Compression tests

4.1 Stress-strain curves

The stress – strain σ - ε diagrams for the 3 wallettes are shown in Fig. 8, where the strain values were obtained through DIC and post-processed in MATLAB. The specimens exhibited an approximately linear behaviour up to the maximum load with a brittle failure.

The mean value σ_m, Young's modulus determined at 1/3 of maximum stress E_i and Poisson's ratio ν of the wallettes are summarized in Table 7. The mean value of σ_m was approximately 2 N/mm^2.

4.2 Full field strain maps

The DIC allowed recovering the complete deformation field at each point of the wall. The evolution in time of the vertical displacement s_y, the vertical strain ε_y and the shear strain γ_{xy}, are shown in three distinct frames (Fig. 9) corresponding to the three highlighted points of Fig. 8.

From the evolution of s_y it could be noted that the wall behaves as a series of independent slender adjacent columns (Fig. 9a). Indeed, the alignment of the vertical joints avoids the uniform downward distribution of the load. This behavior leads to a modest out-of-plane instability phenomenon (confirmed by the 3D-DIC), which is mitigated by the presence of the dovetail joints. The "column effect" is also visible by the evolution of the γ_{xy} that registered high relative sliding between the vertical members (Fig. 9b). As expected, the ε_y is uniformly distributed on the ROI surface with some evident areas of strain concentration (Fig. 9c).

4.3 Full field cracks map

The cracks map under uniaxial compression load obtained through a visual survey is compared with the Von Mises strain map obtained by DIC, in Fig. 10. The cracks propagated from the upper region of the specimens along the masonry surface, with clay expulsions in proximity of the applied force.

The DIC results confirm those obtained by visual inspection and highlight more in detail the weak points. Some vertical cracks, not referable to typical tensile block failures, are located in the proximity of the wall top edge due to an expulsion mechanism.

5. Diagonal compression tests

5.1 Stress-strain curves

The shear stress–strain $\tau - \gamma$ curves for the 3 wallettes are presented in Fig. 11. It can be noted a distinctive yield point when elasticity of the specimen is exceeded and first cracks appeared. The tensile strength τ_m, shear modulus G and shear strain γ of the wallettes are reported in Table 8. The diagonal compression test registered a very low average strength value τ_m (0.002 N/mm^2). This value is due to the specific construction technique which relies only on the friction between the horizontal and the vertical dovetail joints since the thin mortar layer is characterized by low resistance.

5.2 Full field strain maps

The evolution in time of s_x, s_y and γ_{xy}, is illustrated for three distinct moments (see Fig. 12) corresponding to the three highlighted points of Fig. 11. The s_x and s_y maps show that the specimen open up in two parts laterally facing the loading line. This behavior is due to the low adhesion at the interface between the blocks (Fig.12a, b). Additionally, sliding along the joint lines was also visible from the γ_{xy} maps (Fig.12c).

5.3 Full field cracks map

The cracks map under a diagonal compression load derived from a visual inspection is presented in Fig. 13 and is compared with the Von Mises strain map obtained by DIC. All the specimens exhibited a brittle behavior. Fragile-type cracks originated very close to the normal loading line and propagated through the joints, without damaging the blocks. At the end of the tests, all the wallettes were completely disrupted. The DIC successfully reproduced the visual inspection, giving adjunctive information on the strain field.

6. Shear tests with pre-compression

6.1 Stress-strain curves

The results of the shear stress–strain τ-γ diagrams for the 3 specimens subject to a pre-compression load of 0.2 N/mm^2 are presented in Fig. 14. In the first part, the curves showed a linear trend until the first crack appeared. Then, a plastic region occurred with formation of other diagonal cracks. The trend showed a ductile behaviour, typical of shear tests with pre-compression. The tensile strength τ_m, shear modulus G and shear strain γ of the wallettes are collected in Table 9. As expected, the test showed a slight increase (about 2.4%) in terms of tensile strength with respect to the diagonal tensile findings without pre-compression.

6.2 Full field strain maps

The evolution in time of s_x, s_y and γ_{xy} for the wallettes under shear combined with pre-compression are shown in Fig. 16. As expected, the displacement s_x presented an approximately linear trend along the vertical axis (Fig. 15a). The displacement s_y showed a relevant sliding along the vertical joints. This phenomenon has already been pointed out in the full strain maps of the compression test (Fig. 15b). In the strain γ_{xy} maps, two inclined crack lines originating from the point of application of the shear force were visible (Fig. 15c).

6.3 Full field cracks map

The hand-drawn cracks map of the specimens under shear and constant compression load is compared with the Von Mises strain map in Fig. 16. As expected, the failure mechanism highlights diagonal staggered fractures following the vertical and horizontal lines of the joints.

7. Discussion

The present research experimentally investigated through DIC the mechanical behaviour of a new earth block masonry, characterized by industrially extruded units assembled in vertical columns, connected by dovetail joints, and with staggered horizontal bed joints. In particular, the objective was to verify the shear performance and the possible load bearing functions.

The data have proved that the masonry units have low compressive strength, typical of earthen blocks. The average net compressive strength σ_m of the single unit (earth block with dovetail joints) was compared in Fig. 17a with the ones of either unbaked bricks with different mixtures.

The f_{cm} values of the present perforated blocks can be compared with the values obtained in literature regarding experimentations on solid blocks, since the net compressive strength excludes the voids influence. The net strength values are similar to those of solid blocks, namely adobe

bricks [36] earth blocks with coarse sand [37] and manually compressed earthen blocks [37], while they are much lower than those achieved by perforated earth blocks with mechanical compression manufacturing techniques [38].

The average tensile strength τ_m parallel to the dovetail joints of the triplet was compared with the ones of several triplet configurations made of different brick and mortar assemblies [39, 40] (Fig. 17b). The low value of the tensile strength of the present technique is comparable with that of other techniques characterized by poor quality mortar.

The values of the average compressive strength σ_m and the Young modulus E_i of the wallettes were compared with the ones of other earth walls (Fig. 18a). The σ_m and E_i values obtained in the present study (1.59 N/mm^2 and 651 N/mm^2, respectively) were comparable with those of the cob wall but significantly lower than the ones of the rammed earth and earth block walls [12-14]. The low compressive strength of the experimented earth wallette is due to: (i) the particular block adopted here, that is perforated, differently by other studies (e.g. [12 and 13]) that surveyed solid block configurations; (ii) the particular assembly technique, which does not provide the uniform downward load distribution.

The tensile strenght τ_m and shear modulus G of the earth wallette, obtained with diagonal compression tests, were compared with the results of the same aforementioned earth masonries in [12-14] (Fig. 18b). As already mentioned, the earth wallette under study, exhibited a scarce shear behaviour. Indeed, the values of tensile strength (0.002 N/mm^2) and shear modulus (8.68 N/mm^2), were the lowest.

The findings were compared with the experimental results by other authors in literature regarding other masonry samples surveyed through DIC (Fig. 19).

The DIC applied on compression tests (see Fig. 10 and Fig. 19a) revealed the absence of tensile block failure characterized by vertical cracks through the blocks that typically occurs under compression in traditional brick masonries (e.g. [41]) and earthen block masonries with horizontal courses (e.g. [13]). This behaviour is due to the lack in the present wall of a deformable mortar layer, which causes horizontal tensions within the blocks. Moreover, the crack pattern in the present work reveals also a different failure behaviour respect to the one observed in rammed earth wallettes (see e.g. [14]), characterized by the formation of cone shaped cracks at the upper and lower regions.

The DIC on diagonal compression tests showed the presence of weak planes along the bed joints, as also highlighted by other authors regardless the block material and size (see Fig. 13 and Fig. 19b).

For concrete masonry, the strain accumulation was located along the mortar joints where failure occurred [42]. Also for rammed earth, the DIC allowed to visualizing the fracture lines along the compaction layers [16].

The DIC on shear tests with pre-compression highlighted the formation of cracks along the diagonal compressive strut following the staggered lines of the bed joints (see Fig. 16). The shear tests was also evaluated through DIC in [17], [33] and [43]. The former study found quasi-diagonal cracks in rammed earth walls, while the latter two observed more sharply diagonal cracks for traditional fired clay and concrete masonry, respectively (Fig. 19c).

The results clearly showed the capability of DIC to identify the regions with strains concentrations and therefore to locate the position of eventual failure mechanisms.

8. Conclusion

In this paper, the mechanical properties of a new type of earth blocks masonry have been investigated by means of DIC.

The study of the mechanical behavior of the single block and of the joints gave the following results:

- Compressive strength of the earth block was low (3.5 MPa), but comparable with the values of adobe blocks;
- The tensile strength, evaluated in triplets, was low (0.04 MPa) regardless the presence of the dovetail joints.

The study of the mechanical behavior of 12 wallettes under compression, shear and a combination of them, gave the following results:

- The compression tests highlighted that the geometry of the block coupled with the horizontally staggered wall assembly led to a “column behavior” differently from traditional masonries. During the test, a differential sliding between bricks columns occurred;
- The diagonal compression tests registered a low tensile resistance value since the low quality earth mortar coupled with the joints vertical alignment did not guarantee a proper bond between the blocks thus enhancing the fragile behavior and the assembly disruption.
- The shear tests under pre-compression loads showed the formation of compressive struts typical of masonries and revealed a slight increase in terms of tensile strength with respect to the diagonal tensile findings without pre-compression, due to the collaboration of the dovetail joints.

In general, the study showed the need to improve the mechanical properties of the earth blocks and the connection ability of the dovetail joints to achieve possible bracing capacities of the walls made

with this technology. The DIC technique was successfully implemented to determine the deformation and failure state of the earth blocks masonries. The full-field measurements using DIC technique is promising, especially when the specimens are subject to inelastic deformations. Moreover, the DIC proved its high potential in stress-strain monitoring.

Acknowledgements

The authors thank TON-GRUPPE ® for having provided the material and particularly Eng. Marco Tinti for his support on the wallettes manufacturing.

REFERENCES

[1] D. Allinson and M. Hall, "Hygrothermal analysis of a stabilised rammed earth test building in the UK," Energy Build., vol. 42, no. 6, pp. 845–852, 2010.

[2] P. Taylor and M. B. Luther, "Evaluating rammed earth walls : a case study," Sol. En., vol. 76, pp. 79–84, 2004.

[3] F. Pacheco-Torgal and S. Jalali, "Earth construction: Lessons from the past for future eco-efficient construction," Constr. Build. Mater., vol. 29, pp. 512–519, 2012.

[4] B. V. Venkatarama Reddy and P. Prasanna Kumar, "Embodied energy in cement stabilised rammed earth walls," Energy Build., vol. 42, no. 3, pp. 380–385, 2010.

[5] O. Bayode, Y. Michael, and D. Adedeji, "Review of economic and environmental bene fi ts of earthen materials for housing in Africa," Front. Archit. Res., vol. 6, no. 4, pp. 519–528, 2017.

[6] E. Quagliarini and S. Lenci, "The influence of natural stabilizers and natural fibres on the mechanical properties of ancient Roman adobe bricks," J. Cult. Herit., vol. 11, no. 3, pp. 309–314, 2010.

[7] V. Sharma, B. M. Marwaha, and H. K. Vinayak, "Enhancing durability of adobe by natural reinforcement for propagating sustainable mud housing," Int. J. Sustain. Built Environ., vol. 5, no. 1, pp. 141–155, 2016.

[8] K. Ghavami, D. T. Filho, and N. P. Barbosac, “Cement & Concrete Composites Behaviour of composite soil reinforced with natural fibres,” Cement and concrete composites, vol. 21, pp. 39–48, 1999.

[9] Ş. Yetgin, Ö. Çavdar, and A. Çavdar, “The effects of the fiber contents on the mechanic properties of the adobes,” Constr. Build. Mater., vol. 22, no. 3, pp. 222–227, 2008.

[10] H. Binici, O. Aksogan, and T. Shah “Investigation of fibre reinforced mud brick as a building material,” Constr. Build. Mat., vol. 19, pp. 313–318, 2005.

[11] C. H. Kouakou and J. C. Morel, “Applied Clay Science Strength and elasto-plastic properties of non-industrial building materials manufactured with clay as a natural binder,” Appl. Clay Sci., vol. 44, no. 1–2, pp. 27–34, 2009.

[12] L. Miccoli, U. Müller, and P. Fontana, “Mechanical behaviour of earthen materials: A comparison between earth block masonry, rammed earth and cob,” Constr. Build. Mater., vol. 61, pp. 327–339, 2014.

[13] L. Miccoli, A. Garofano, P. Fontana, and U. Müller, “Experimental testing and finite element modelling of earth block masonry,” Eng. Struct., vol. 104, pp. 80–94, 2015.

[14] L. Miccoli, D. V. Oliveira, R. A. Silva, U. Müller, and L. Schueremans, “Static behaviour of rammed earth: experimental testing and finite element modelling,” Mater. Struct. Constr., 2015.

[15] D. Maskell, A. Heath, and P. Walker, “Laboratory scale testing of extruded earth masonry units,” J. Mater., vol. 45, pp. 359–364, 2013.

[16] R. A. Silva, O. Domínguez-martínez, D. V Oliveira, and E. B. Pereira, “Comparison of the performance of hydraulic lime-and clay-based grouts in the repair of rammed earth,” Constr. Build. Mater., vol. 193, pp. 384–394, 2018.

[17] R. El-nabouch, Q. Bui, O. Plé, and P. Perrotin, “Assessing the in-plane seismic performance of rammed earth walls by using horizontal loading tests,” Eng. Struct., vol. 145, pp. 153–161, 2017.

[18] N. McCormick and J. Lord, “Digital image correlation,” Mater. Today, vol. 13, no. 12, pp. 52–54, 2010.

[19] M. Di Benedetti, S. Cholostiakow, H. Fergani, E. Zappa, A. Cigada, and M. Guadagnini “3D-DIC for strain measurement in small scal GFRP RC specimens”, Proceedings of SMAR

2015, 3rd conference on smart monitoring, Antalaya, Turkey .

[20] M. Tekieli, S. De Santis, G. de Felice, A. Kwiecień, and F. Roscini, "Application of Digital Image Correlation to composite reinforcements testing," Compos. Struct., vol. 160, pp. 670–688, 2017.

[21] C. Caggegi, D. Sciuto, and M. Cuomo, "Experimental study on effective bond length of basalt textile reinforced mortar strengthening system: Contributions of digital image correlation," Meas. J. Int. Meas. Confed., vol. 129, no. June, pp. 119–127, 2018.

[22] B. Ghiassi, J. Xavier, D. V Oliveira, A. Kwiecien, and P. B. Lourenço, "Evaluation of the bond performance in FRP – brick components re-bonded after initial delamination," Compos. Struct., vol. 123, pp. 271–281, 2015.

[23] D. Markulak, T. Dokšanović, I. Radić, and I. Miličević, "Structurally and environmentally favorable masonry units for infilled frames," Eng. Struct., vol. 175, no. March, pp. 753–764, 2018.

[24] M. A. Sutton, F. Matta, D. Rizos, R. Ghorbani, S. Rajan, and D. H. Mollenhauer, "Recent Progress in Digital Image Correlation : Background and Developments since the 2013 W M Murray Lecture," Exp. Mech., pp. 1–30, 2017.

[25] N. Guerrero, M. Martinez, R. Picòn, M.E. Marante, F. Hild, and S. Roux, "Experimental analysis of masonry infilled frames using digital image correlation," Mater. Struct., vol. 47, no. 5, pp. 873–884, 2014.

[26] R. Ghorbani, F. Matta, and M. A. Sutton, "Full-Field Deformation Measurement and Crack Mapping on Confined Masonry Walls Using Digital Image Correlation," Exp. Mech., vol. 55, no. 1, pp. 227–243, 2015.

[27] E. Speranzini, R. Marsili, M. Moretti, and G. Rossi, "Image Analysis Technique for Material Behavior Evaluation in Civil Structures," Materials (Basel)., vol. 10, no. 7, p. 770, 2017.

[28] D. Amodio, G. B. Broggiato, E. Campana, and G. M. Newaz, "Digital Speckle Correlation for Strain Measurement by Image Analysis," Exp. Mech., vol. 43, no. 4, pp. 396–402, 2003.

[29] G. Chiappini, M. Sasso, T. Bellezze, and D. Amodio "Thermo-structural analysis of components in ceramic material," Procedia Struct. Integr., vol. 8, pp. 618–627, 2018.

[30] F. Stazi, F. Tittarelli, F. Saltarelli, G. Chiappini, A. Morini, G. Cerri, and S. Lenci, "Carbon nano fibers in polyurethane foams : Experimental evaluation of thermo-hygrometric and

mechanical performance," Pol. Test., vol. 67, no. September 2017, pp. 234–245, 2018.

[31] M. Sasso, E. Mancini, G. Chiappini, F. Sarasini and J. Tirillò "Application of DIC to Static and Dynamic Testing of Agglomerated Cork Material," Exp. Mech., pp. 1017–1033, 2018.

[32] J. Donnini, G. Chiappini, G. Lancioni, and V. Corinaldesi, "Tensile behaviour of glass FRCM systems with fabrics' overlap : Experimental results and numerical modeling," Compos. Struct., vol. 212, no. January, pp. 398–411, 2019.

[33] S. Tung and M. Shih, "Development of digital image correlation method to analyse crack variations of masonry wall," vol. 33, no. December, pp. 767–779, 2008.

[34] E. Quagliarini, S. Lenci, and M. Iorio, "Mechanical properties of adobe walls in a Roman Republican domus at Suasa," J. Cult. Herit., vol. 11, no. 2, pp. 130–137, 2010.

[35] H. U. Sajid, M. Ashraf, Q. Ali, and S. H. Sajid, "Effects of vertical stresses and flanges on seismic behavior of unreinforced brick masonry," Eng. Struct., vol. 155, no. April 2017, pp. 394–409, 2018.

[36] R. Illampas, I. Ioannou, and D. C. Charmpis, "Adobe bricks under compression : Experimental investigation and derivation of stress – strain equation," Constr. Build. Mater., vol. 53, pp. 83–90, 2014.

[37] Q. Piattoni, E. Quagliarini, and S. Lenci, "Experimental analysis and modelling of the mechanical behaviour of earthen bricks," Constr. Build. Mater., vol. 25, no. 4, pp. 2067–2075, 2011.

[38] J. D. Sitton, Y. Zeinali, W. H. Heidarian, and B. A. Story, "Effect of mix design on compressed earth block strength," Constr. Build. Mater., vol. 158, pp. 124–131, 2018.

[39] V. Alecci, M. Fagone, T. Rotunno, and M. De Stefano, "Shear strength of brick masonry walls assembled with different types of mortar," Constr. Build. Mater., vol. 40, pp. 1038–1045, 2013.

[40] V. Corinaldesi and G. Moriconi, "Behaviour of cementitious mortars containing different kinds of recycled aggregate," Constr. Build. Mater., vol. 23, no. 1, pp. 289–294, 2009.

[41] K. Willam, A. Mohammadipour, R. Mousavi, and A. S. Ayoub, "Failure of Unreinforced Masonry Under Compression," Structures congress 2013, pp. 2949–2961, 2013.

[42] F. Khan, A. Kontsos, I. Bartoli, and M. Bolhassani, "Using DIC to measure deformation

fields of concrete masonry test specimens," 12th Canadian Masonry Symposium, June, 2013.

[43] F. Khan, R. Carmi, S. Rajaram, and M. Bolhassani, "Multiple cross validated sensing system for damage monitoring in civil structural components" Proceedings of the 9 th International Workshop on Structural Health Monitoring 2013, January, 2013.

List of captions

Fig. 1. (a) Earth block geometry, (b) Platform-Frame construction system and (c)external envelope layers.

Fig. 2. Grain size distribution of the soil matrix.

Fig. 3. Tests set up for (a) the determination of the compressive strength of the earth block, (b) the determination of the initial shear strength parallel to the dovetail joints (configuration A) and (c) the determination of the initial shear strength perpendicular to the dovetail joints (configuration B).

Fig. 4. DIC set up.

Fig. 5. (a) Picture whit overlaid grid, (b) 3D grid point, and (c) strain noise evaluation for the 3D-DIC.

Fig. 6. Tests set up of the wallette specimen for (a) the determination of its compressive strength, (b) the determination of its tensile strength and (c) the determination of its shear strength with a constant compression load.

Fig. 7. Failure modes of (a) the earth block, (b) of the triplet (configuration A) and (c) of the triplet (configuration B).

Fig. 8. $\sigma - \varepsilon$ curves of the wallette specimens under compression load.

Fig. 9. Complete displacement and strains fields of the wallettes under compression load.

Fig. 10. Crack mapping on wallette under compression load: (a) Von Mises strain field of the ultimate state and (b) hand-drawn map based on visual inspection.

Fig. 11. τ-γ curves of the wallette specimens under diagonal compression load.

Fig. 12. Complete displacements and strain fields of the wallettes under diagonal compression load.

Fig. 13. Crack mapping on wallette diagonal compression load: (a) Von Mises strain field of the ultimate state and (b) hand-drawn map based on visual inspection.

Fig. 14. τ-γ curves of the wallette specimen under a shear and constant compression of 0.2 N/(mm^2).

Fig. 15. Complete displacements and strain fields of the wallettes under a shear and constant compression of 0.2 N/(mm^2).

Fig. 16. Crack mapping on wallette under shear and pre-compression load: (a) Von Mises strain field of the ultimate state and (b) hand-drawn map based on visual inspection.

Fig. 17. Comparison of (a) the compressive strength values of different types of bricks and (b) of the initial shear strength of triplet setups.

Fig. 18. Comparison of (a) the compressive strengths, and (b) the tensile strengths of different types of masonries obtained from a diagonal compression load.

Fig. 19. Results of the DIC technique applied in masonries under (a) compression load, (b) diagonal compression load and (c) shear with pre-compression.

Tables

Table 1. Overview of the lab tests made on wallettes.

Test method	Standard/Reference	Description	Specimen
Determination of compressive strength	UNI EN 1052-1:2001	Application of an evenly distributed load to the cross section of the panel until failure occurs.	n. 3
Determination of diagonal tensile strength	ASTM E519 – 07	Application of an evenly distributed compression load along one diagonal axis.	n. 3
Determination of tensile strength with pre-compression load	[34]	Application of a shear force to a wallette subject to a pre-compression load.	n. 3

Table 2. Main geotechnical characteristics of the soil matrix.

Liquid limit	44%
Plasticity index	23%
Fine (< 75 μm)	100%
Clay (< 2 μm)	22%
Activity	1.05

Table 3. Granulometric and mineralogical properties of the used earthen material

Grain size distribution (wt%)			Mineralogic properties			
			Grain	Clay		
Clay (< 0.002 mm)	Silt (0.002-0.063 mm)	Sand (0.063-2 mm)	Quartz	Illite	Kaolinite	Montmorillonite and Chlorite
42	57	1	+++	++	+	+

Quantities +++ high; ++ medium; + low

Table 4. Optical set-up and calibration parameters.

		CAMERA 1	CAMERA 2	CAMERA 3
Sensor	(Type)	CMOS	CMOS	CMOS
Sensor pixel size	(μm)	6.8 × 6.8	6.8 × 6.8	6.8 × 6.8
Sensor resolution	(pixel)	1280 × 1024	1280 × 1024	1280 × 1024
Frame rate	(fps)	27	27	27
Lens	(Type, mm)	C mount, 16	C mount, 16	C mount, 25
Working distance	(mm)	2000	2000	4000
Sensor noise	(gray level, dB)	0.94, −19	0.94, −19	0.94, −19
Subset size	(pixel, mm)	25, 20	25, 20	20, 20
Displ. accuracy (st. dev)	(pixel, mm)	±(0.05, 0.1)	±(0.05, 0.1)	±(0.08, 0.1)
Strain accuracy (st. dev)	(mm/mm)	±0.0001	±0.0001	±0.00015
CALIBRATION DATA				
fx - fy	(pixel)	1811 - 1803	1818 - 1811	/
cx - cy	(pixel)	659 - 523	708 - 524	/
T_x – T_y - T_z	(mm)	484 – 454 – 2200		/
α_x – α_y - α_z	(rad)	0.0222 – 0.0032 – 0.0198		/

Table 5. Compressive test results of the earth blocks.

Specimen	Avg. net compressive strength f_{cm} (N/mm^2)	SD (N/mm^2)	COV (%)
A1-A9	3.4	0.4	0.12

Table 6. Initial shear strengths of the triplets.

Specimen	Avg. tensile strength f_{vo} (N/mm^2)	Characteristic tensile strength f_{vok} (N/mm^2)	SD (N/mm^2)	COV (%)
T1-T3 parallel	0.04	0.03	0.01	18.6
T1-T3 perpendicular	2.37	1.90	0.14	5.8

Table 7. Compressive strength, Young modulus and normal strain of the wallette.

Specimen	σ (N/mm^2)	E_i (N/mm^2)	γ
C1	2.02	591	0.22
C2	2.46	703	0.23
C3	1.48	740	0.28
σ_m	1.99	678	0.24
SD	0.49	78	0.03
COV	25%	11%	13%

Table 8. Tensile strength, Young modulus and shear strain of the wallette.

Specimen	τ (N/mm^2)	G (N/mm^2)	γ
S1	0.00246	7.76	0.000105718
S2	0.00236	8.09	9.70814E-05
S3	0.00254	10.20	8.26778E-05
τ_m	0.00245	8.68	9.51591E-05
SD	0.00009	1.32	1.16398E-05
COV	4%	105%	12%

Table 9. Tensile strength, shear modulus and shear strain of the wallettes under a precompression load.

Specimen	τ (N/mm^2)	G (N/mm^2)	γ
SP02_1	0.176	35	0.051
SP02_2	0.168	40	0.045
SP02_3	0.157	39	0.056
τ_m	0.167	38	0.051
SD	0.010	3	0.006
COV	5.7%	7.0%	11.2%
SP04_1	0.176	344	0.048
SP04_2	0.171	310	0.035
SP04_3	0.180	329	0.042
τ_m	0.176	327	0.041
SD	0.005	17	0.006
COV	0.027	0	0.148

Figure 1

Click here to download high resolution image

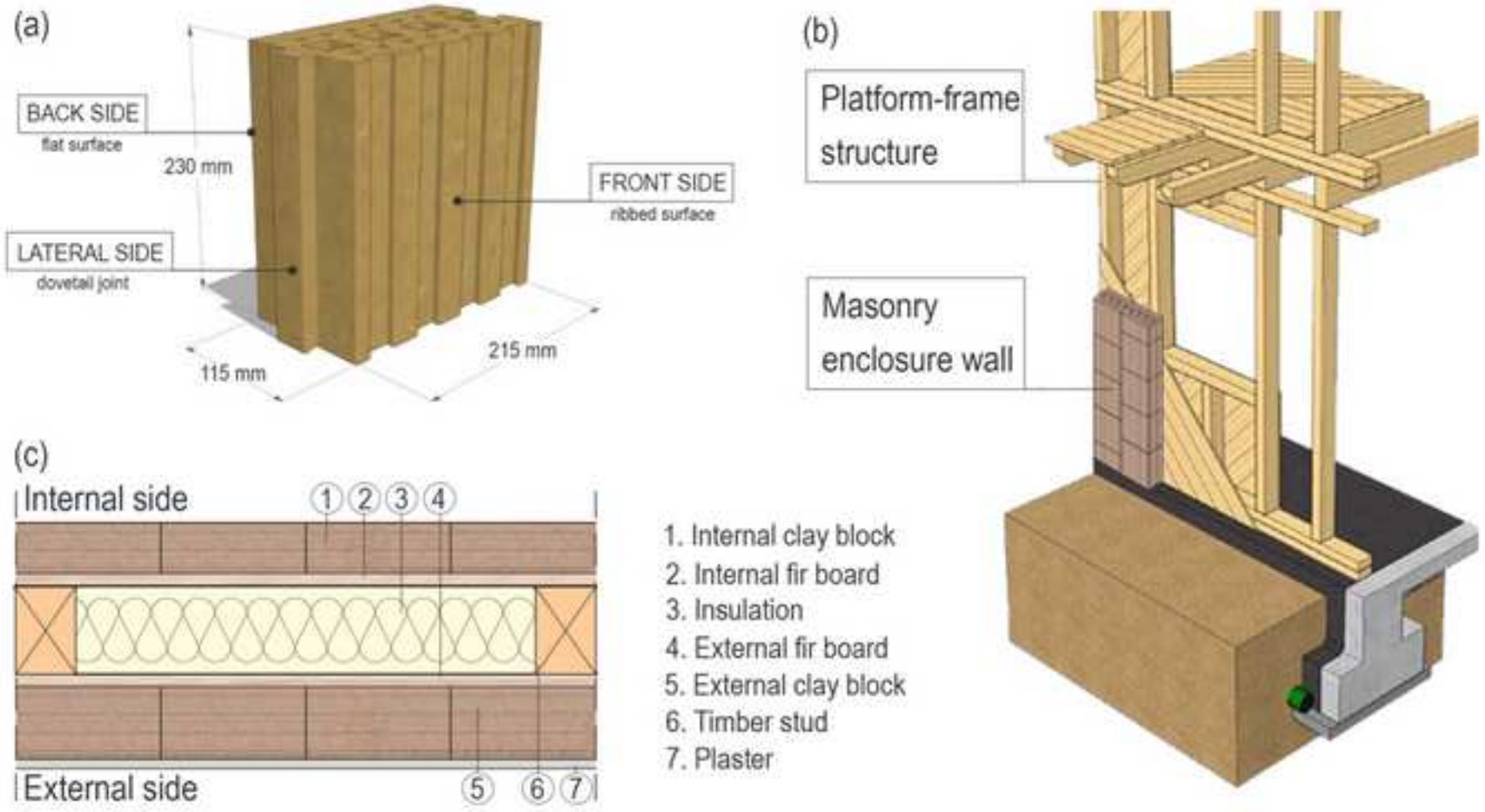

Figure 2

Click here to download high resolution image

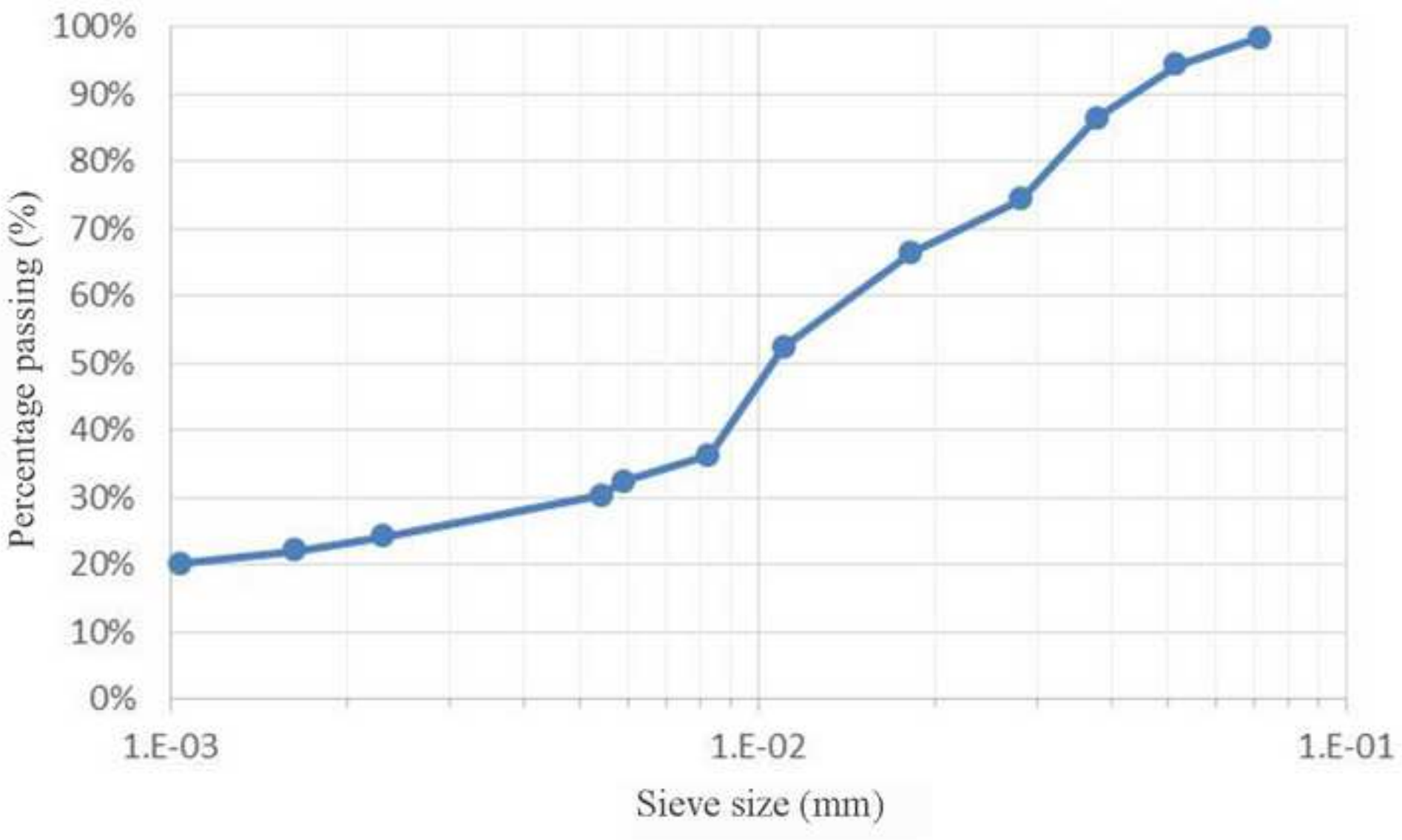

Figure 3
Click here to download high resolution image

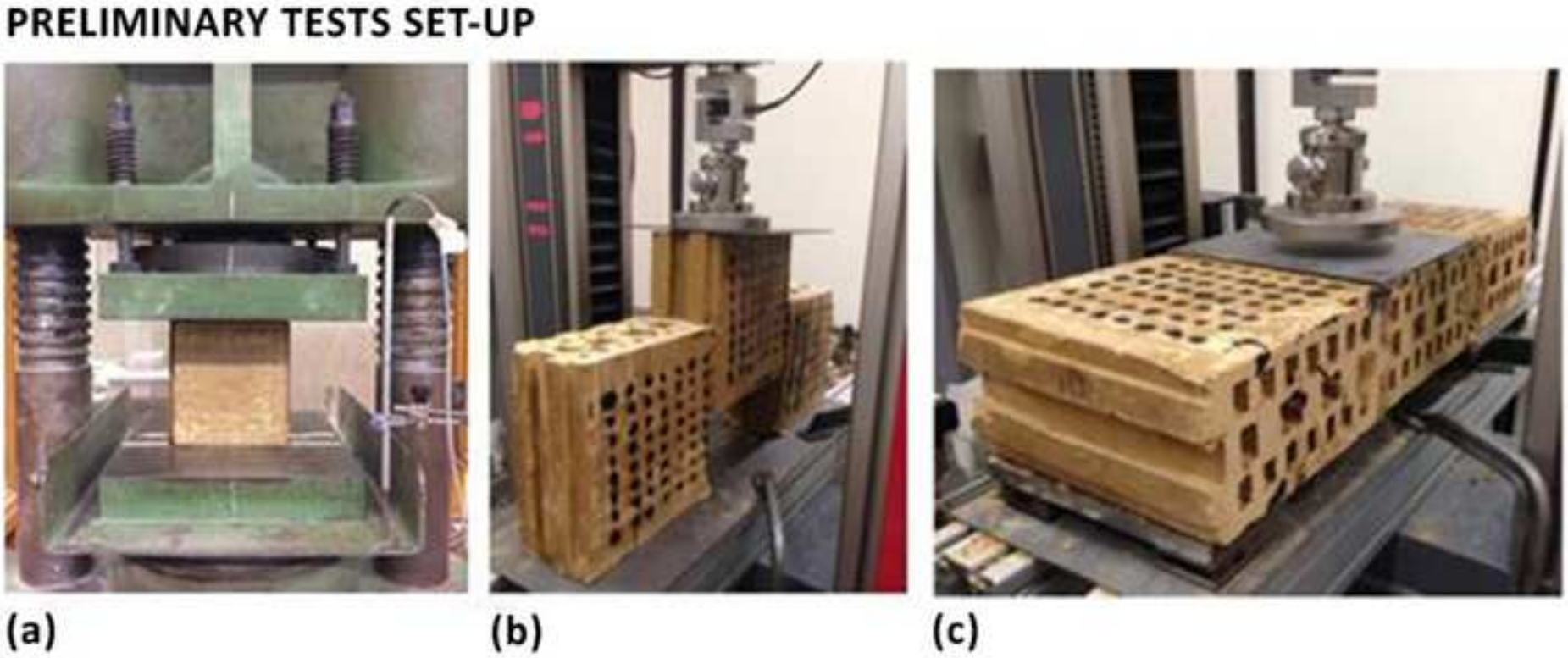

Figure 4

Click here to download high resolution image

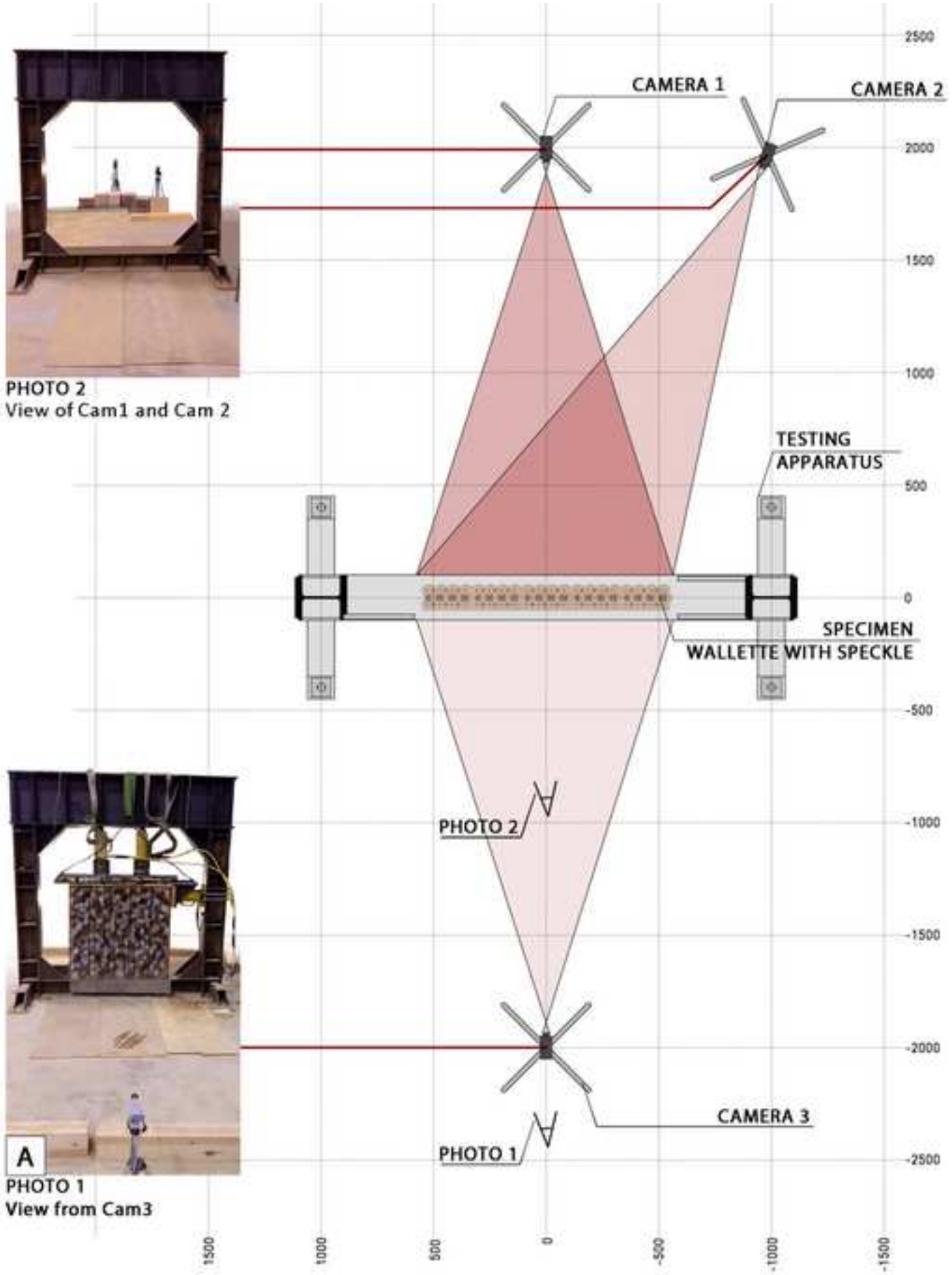

PHOTO 2
View of Cam1 and Cam 2

PHOTO 1
View from Cam3

Figure 5

Click here to download high resolution image

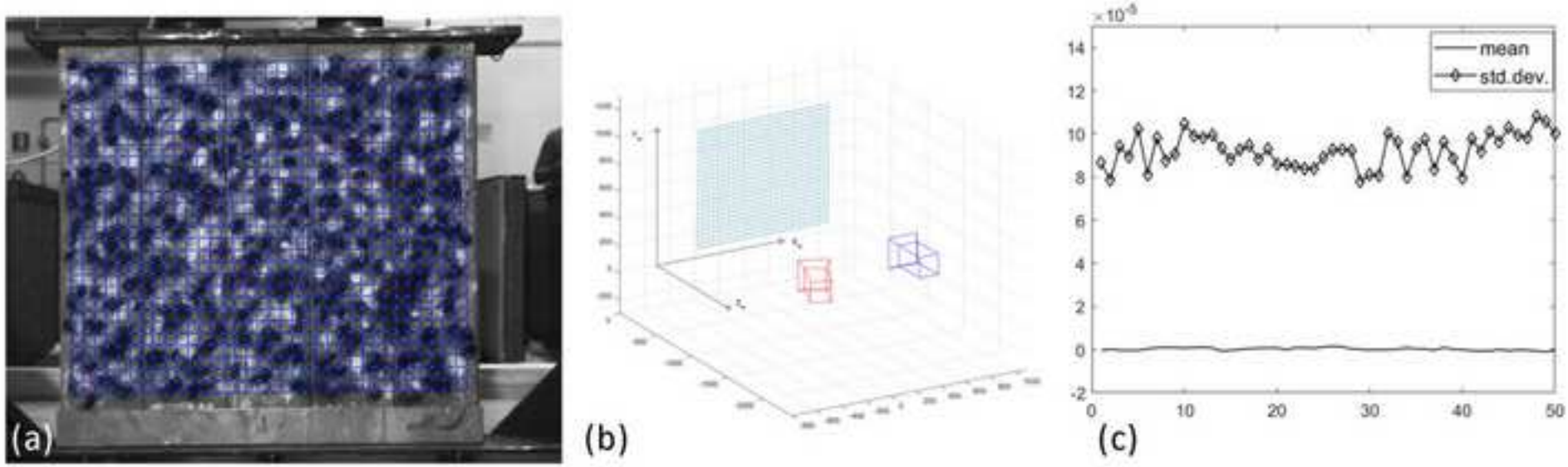

Figure 6

Click here to download high resolution image

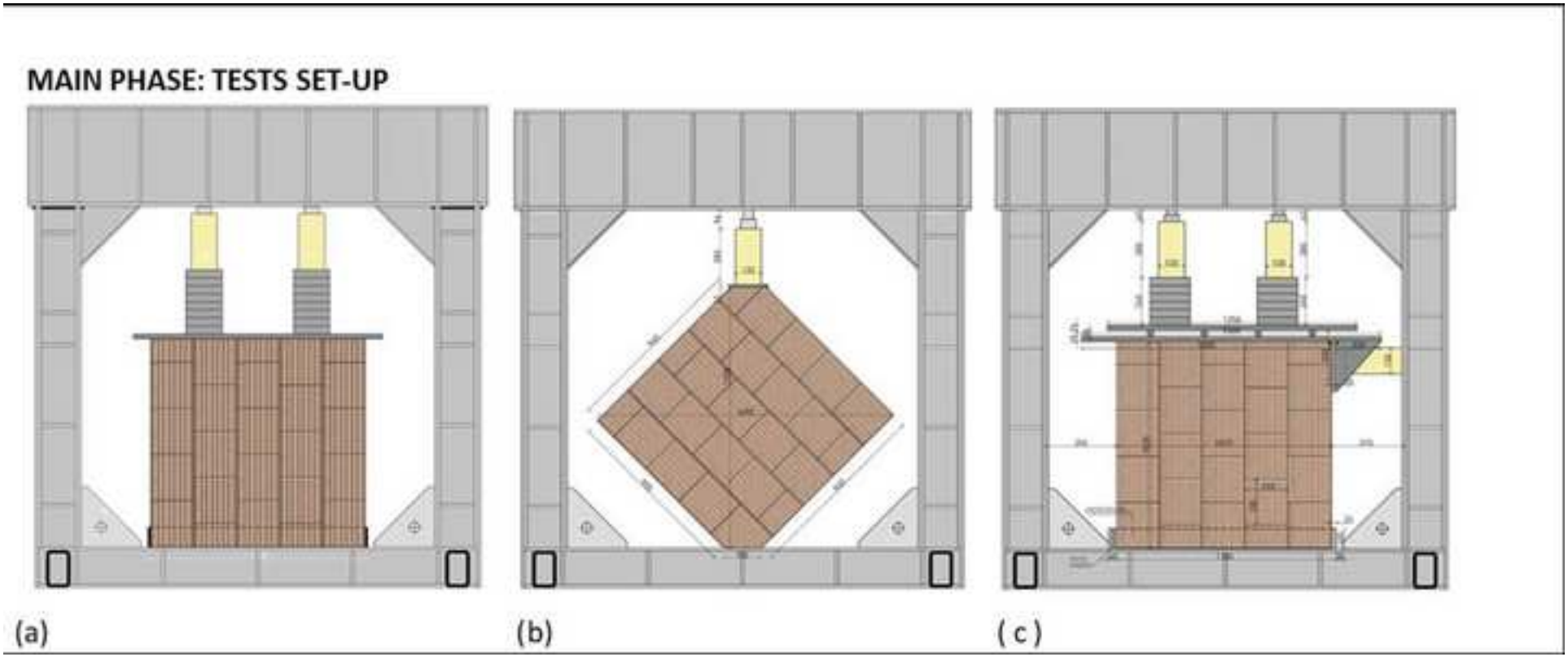

Figure 7
Click here to download high resolution image

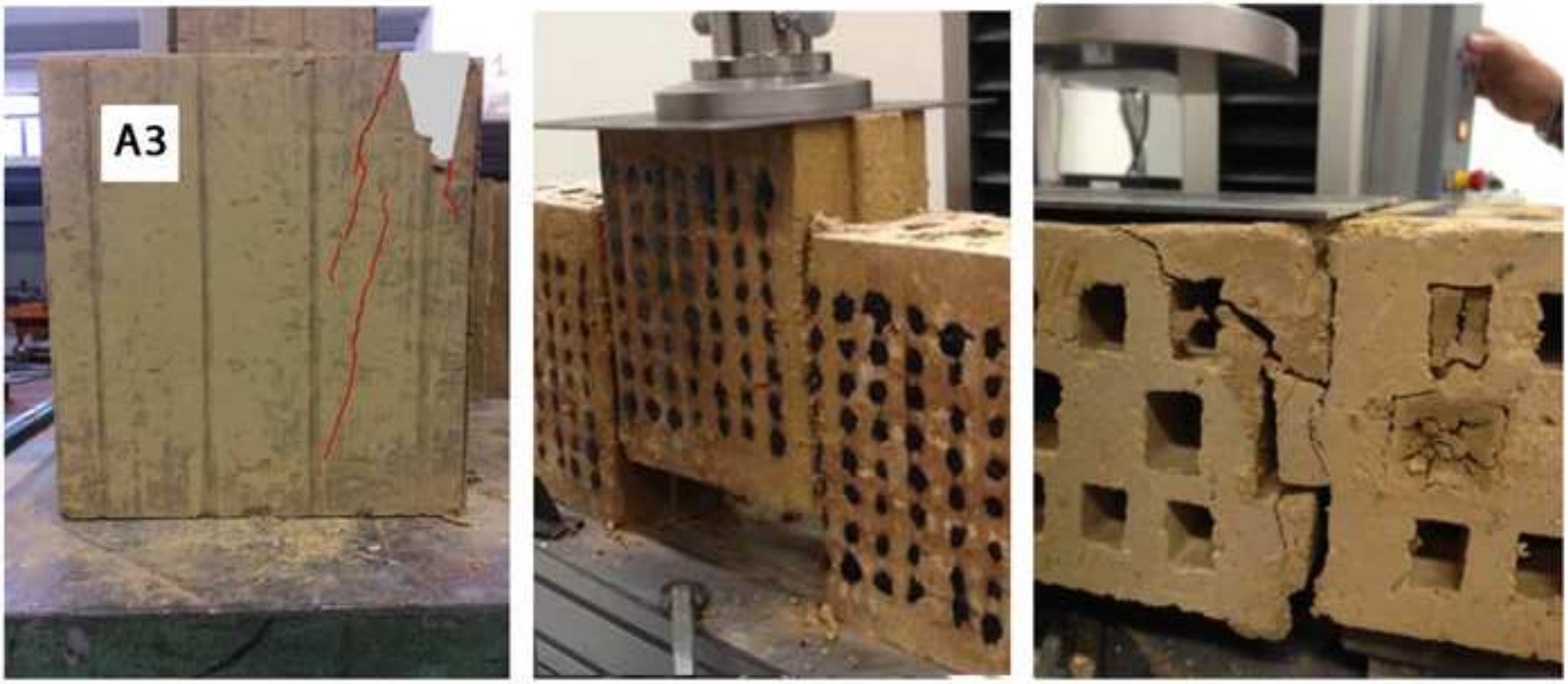

Figure 8

Click here to download high resolution image

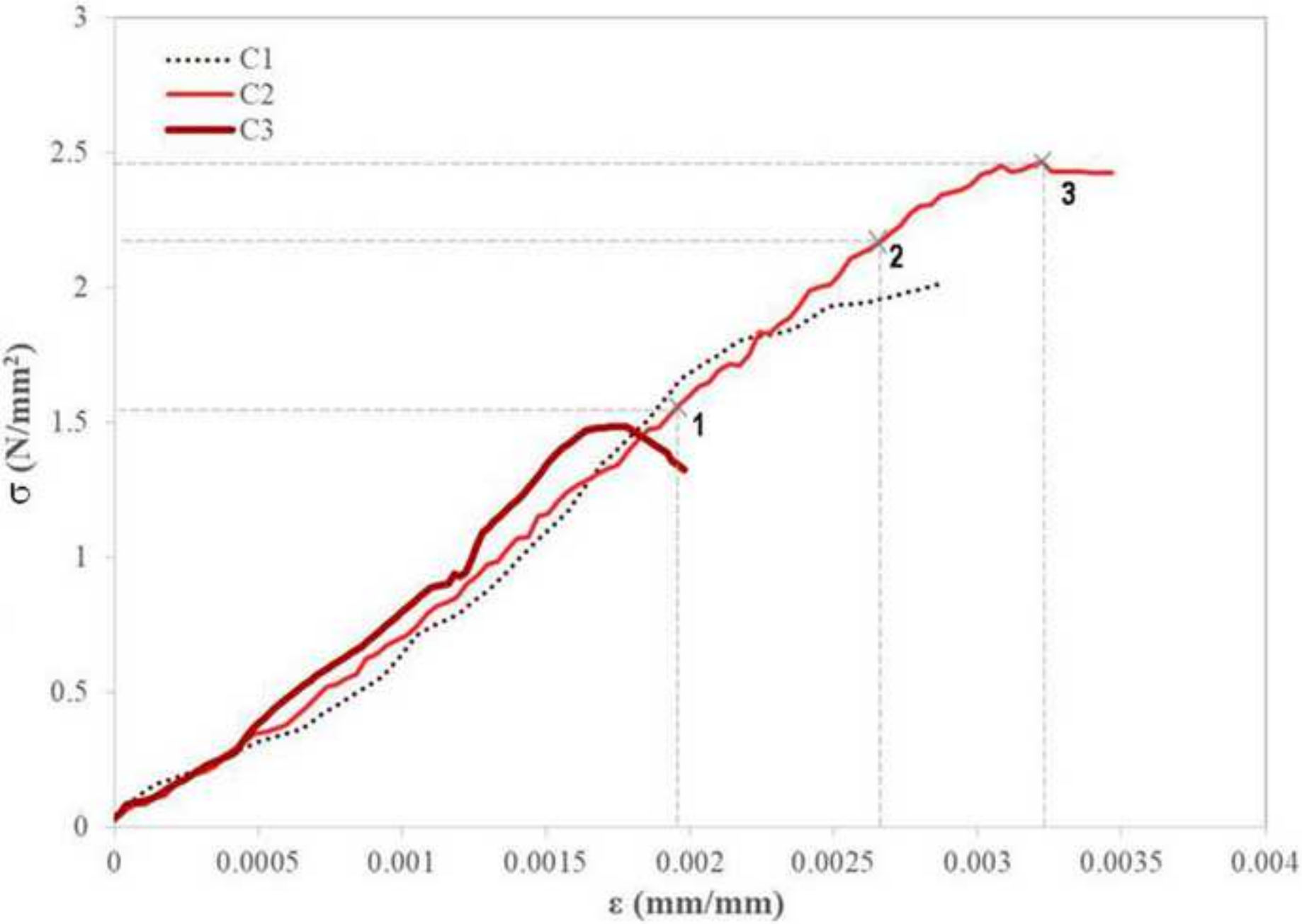

Figure 9

Click here to download high resolution image

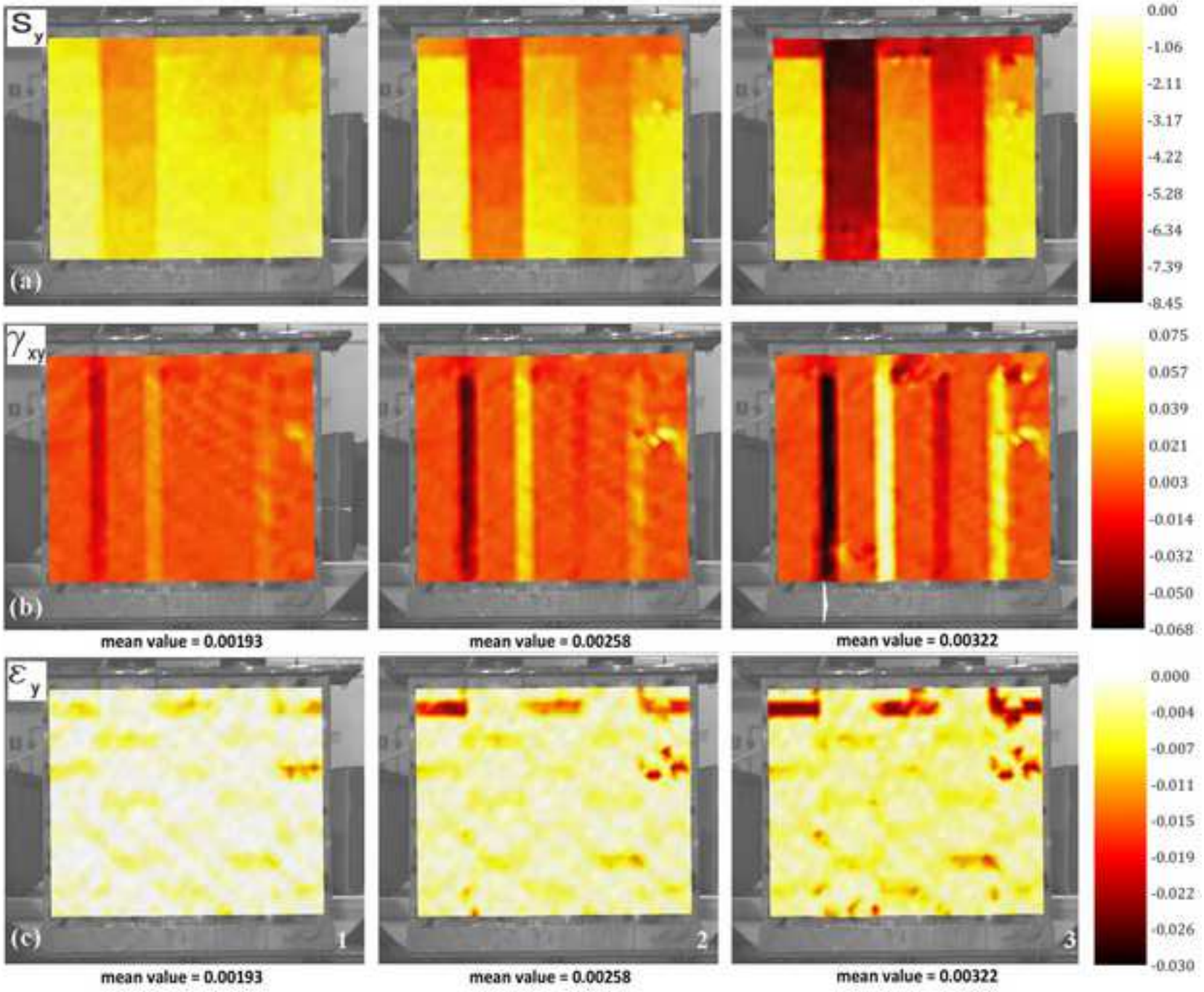

Figure 10

Click here to download high resolution image

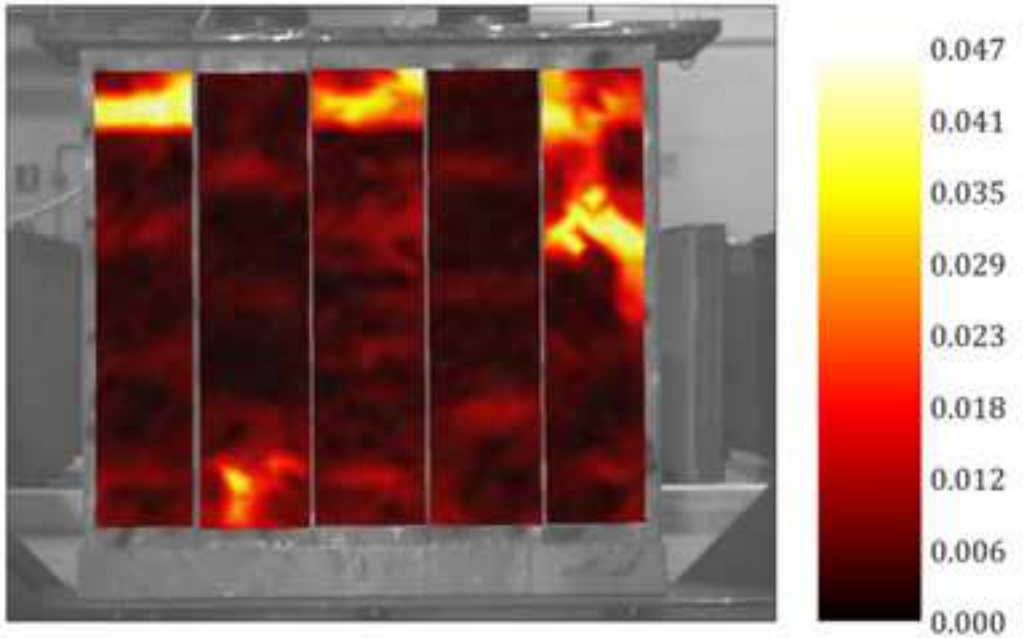

(a) Von Mises strain map

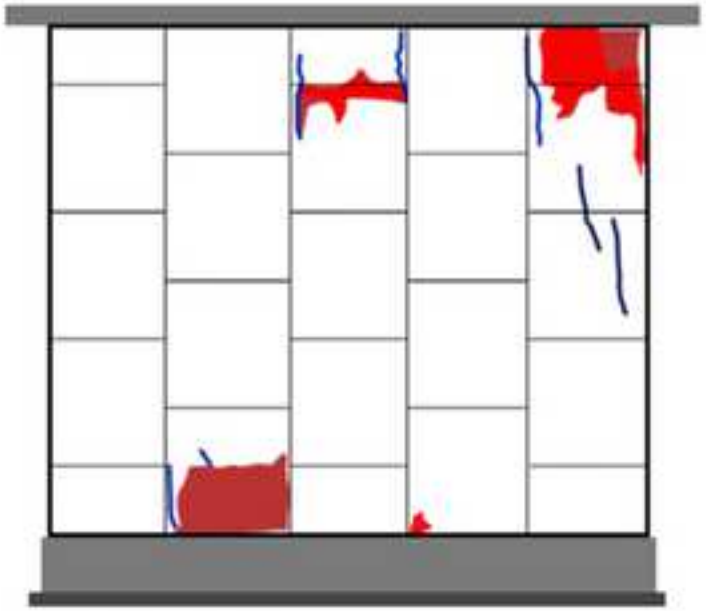

(b) Hand-drawn map

Figure 11

Click here to download high resolution image

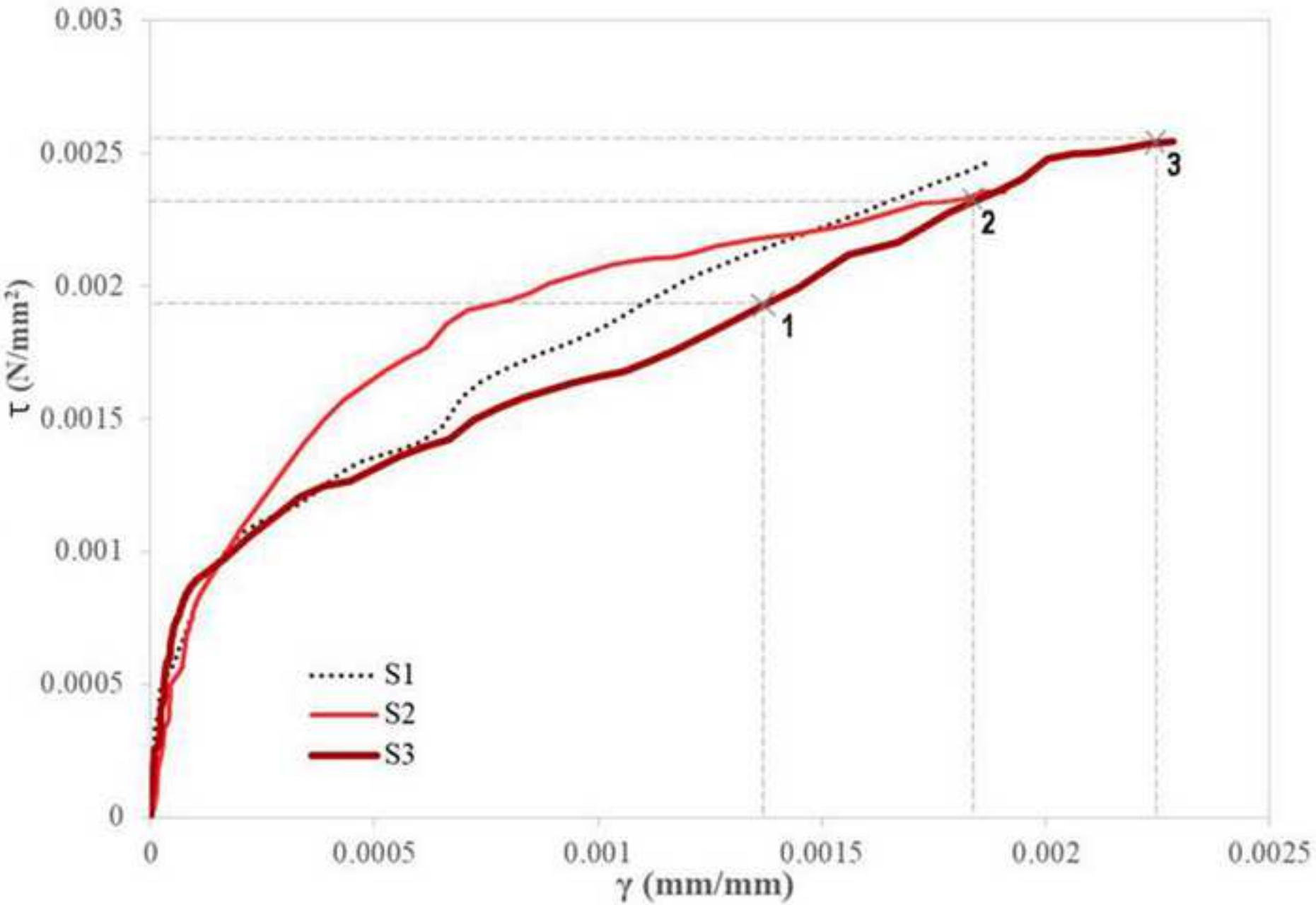

Figure 12

Click here to download high resolution image

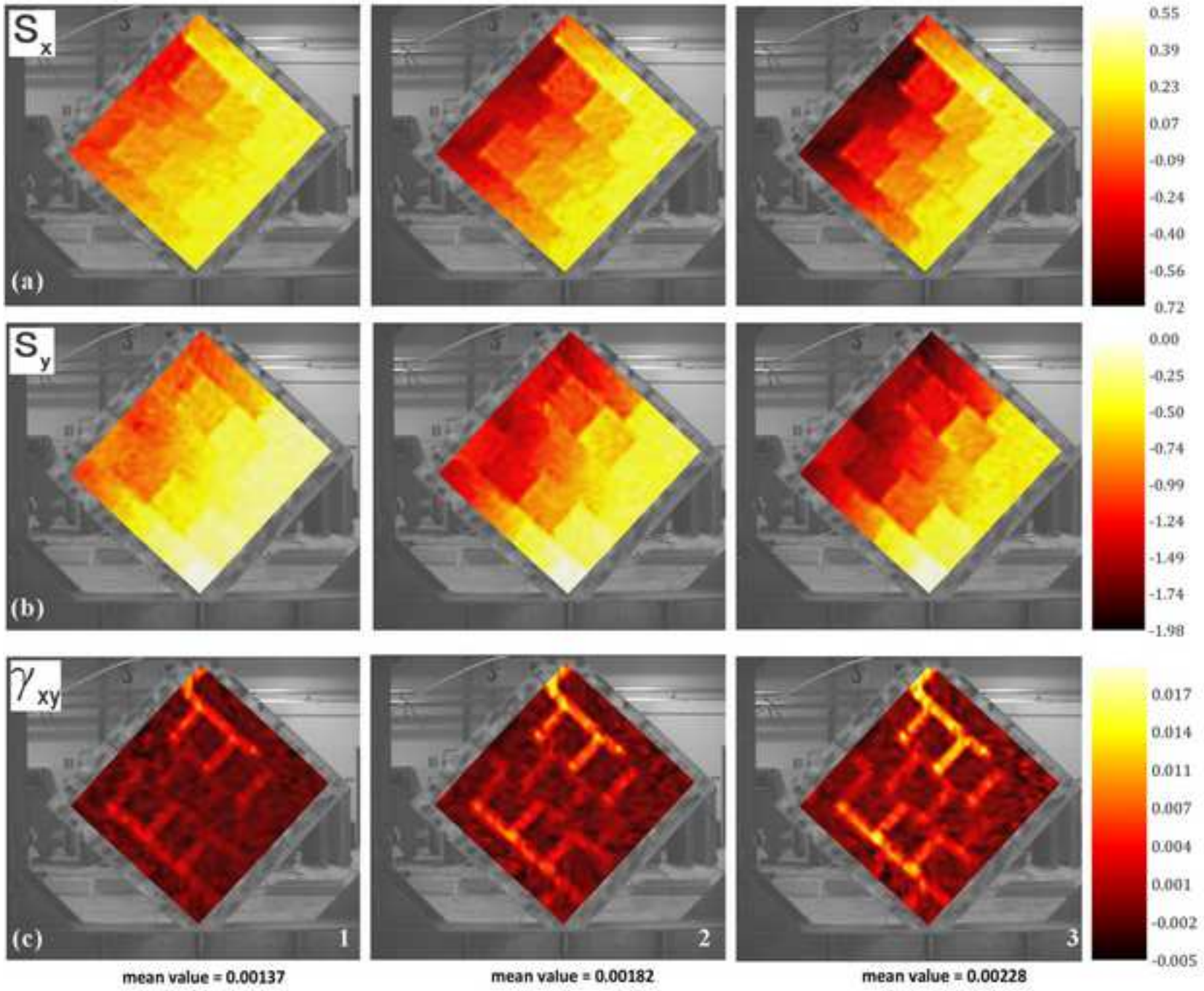

Figure 13
Click here to download high resolution image

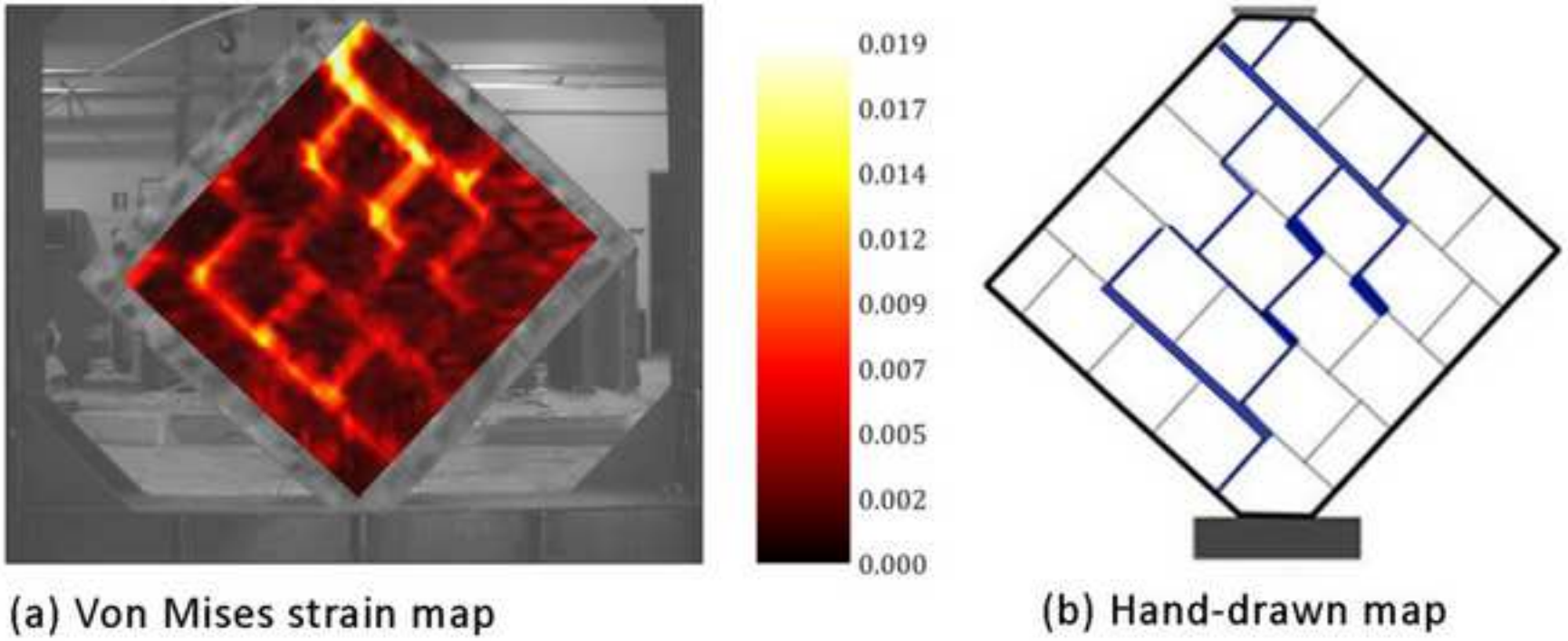

(a) Von Mises strain map

(b) Hand-drawn map

Figure 14

Click here to download high resolution image

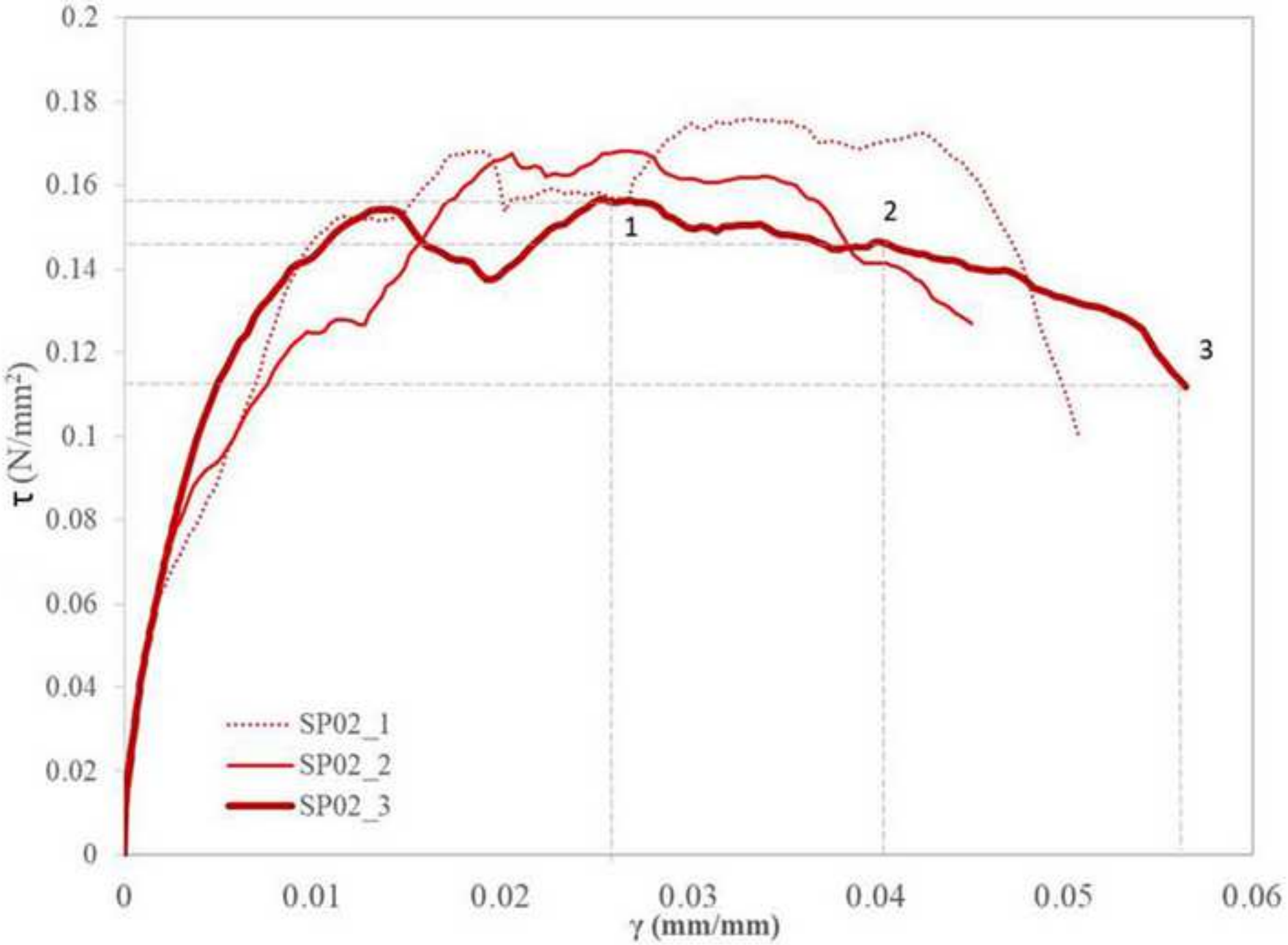

Figure 15

Click here to download high resolution image

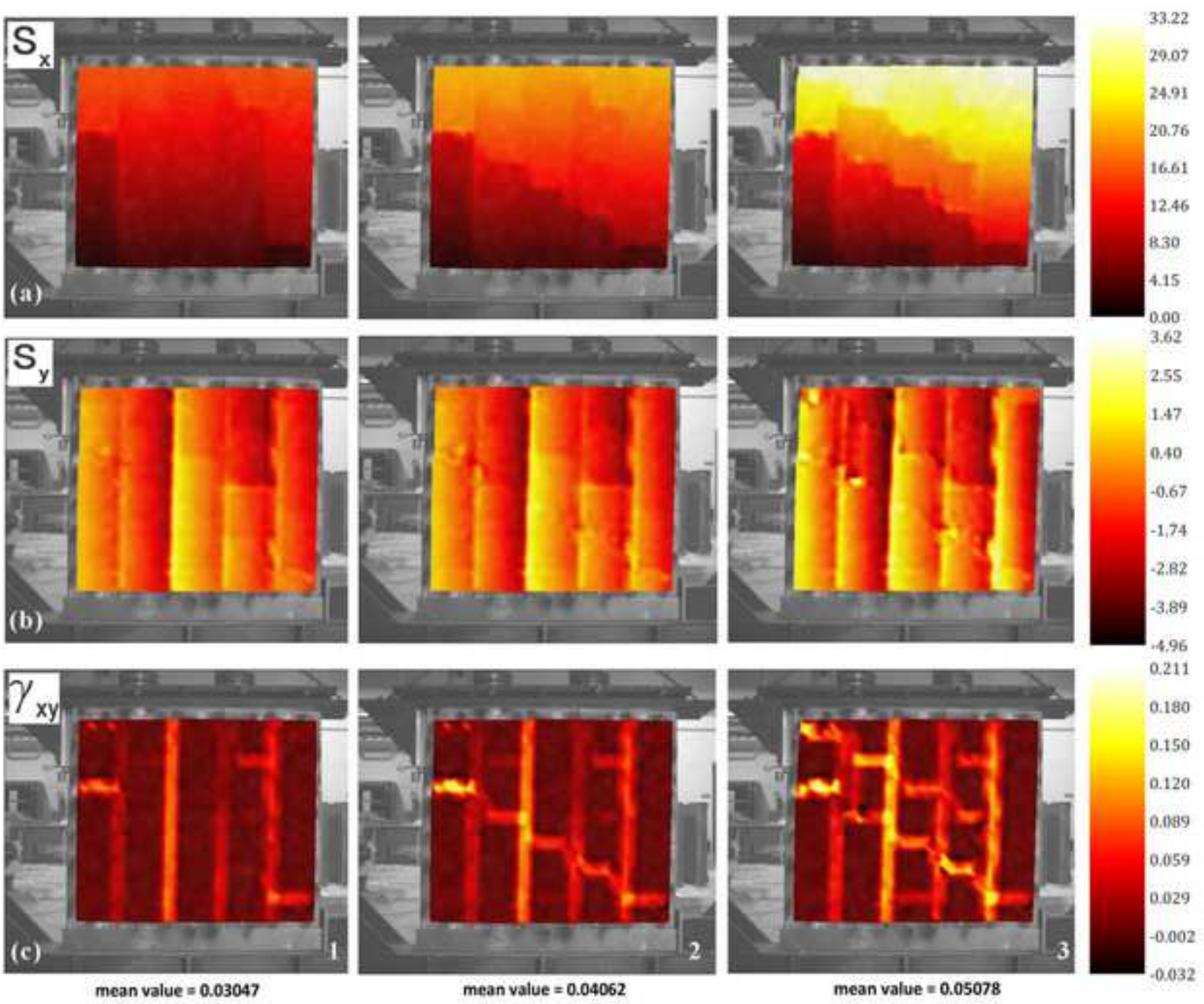

Figure 16
Click here to download high resolution image

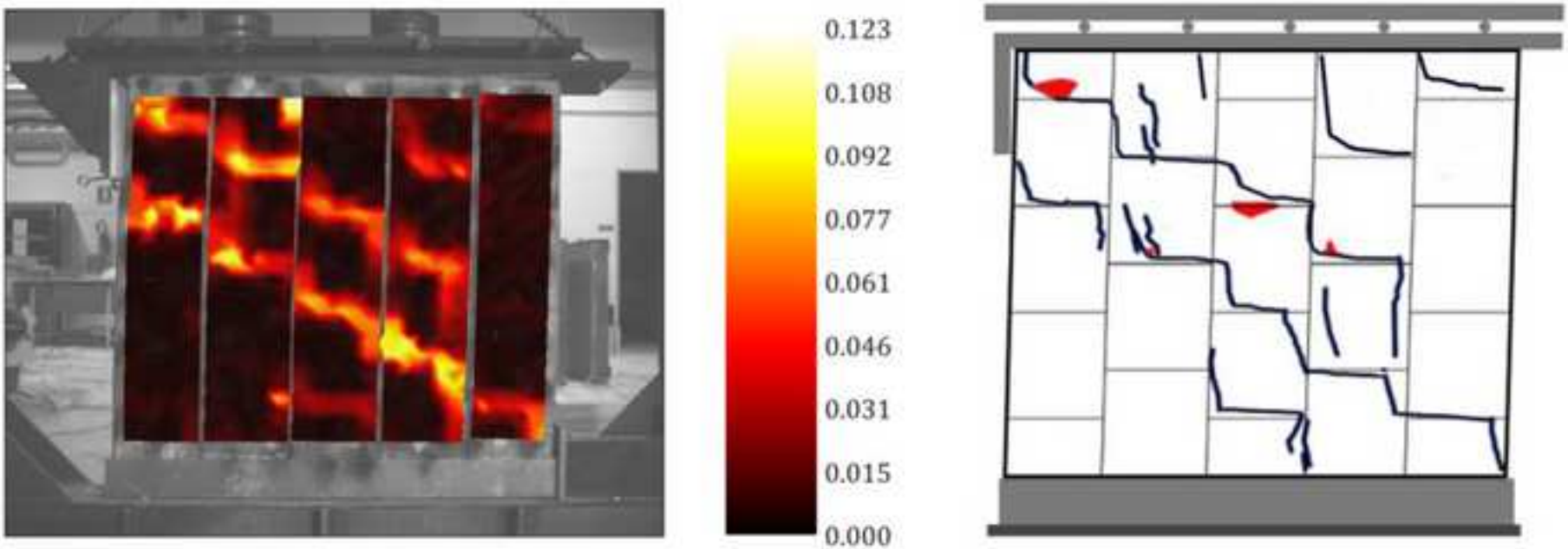

(a) Von Mises strain map

(b) Hand-drawn map

Figure 17

Click here to download high resolution image

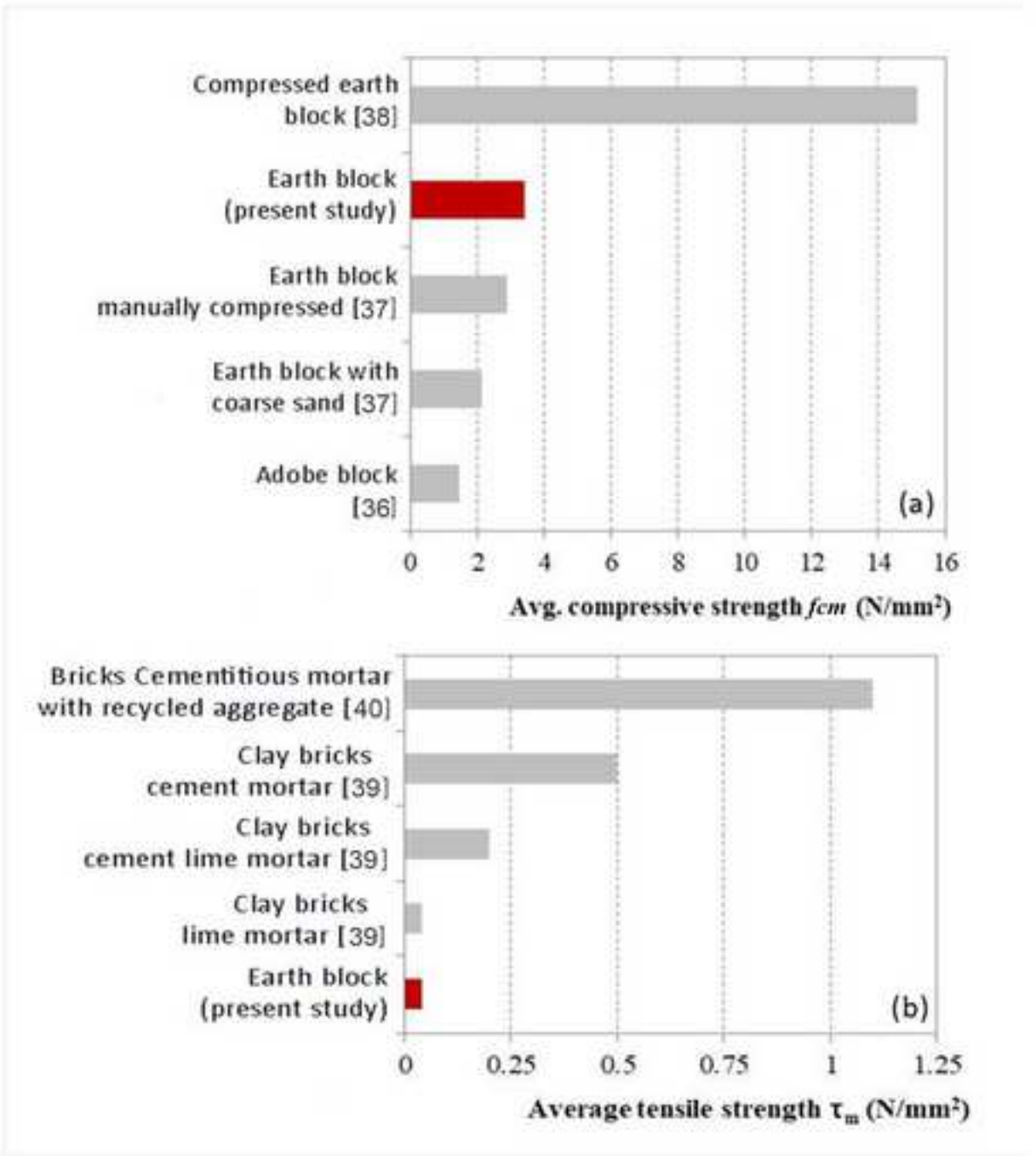

Figure 18
Click here to download high resolution image

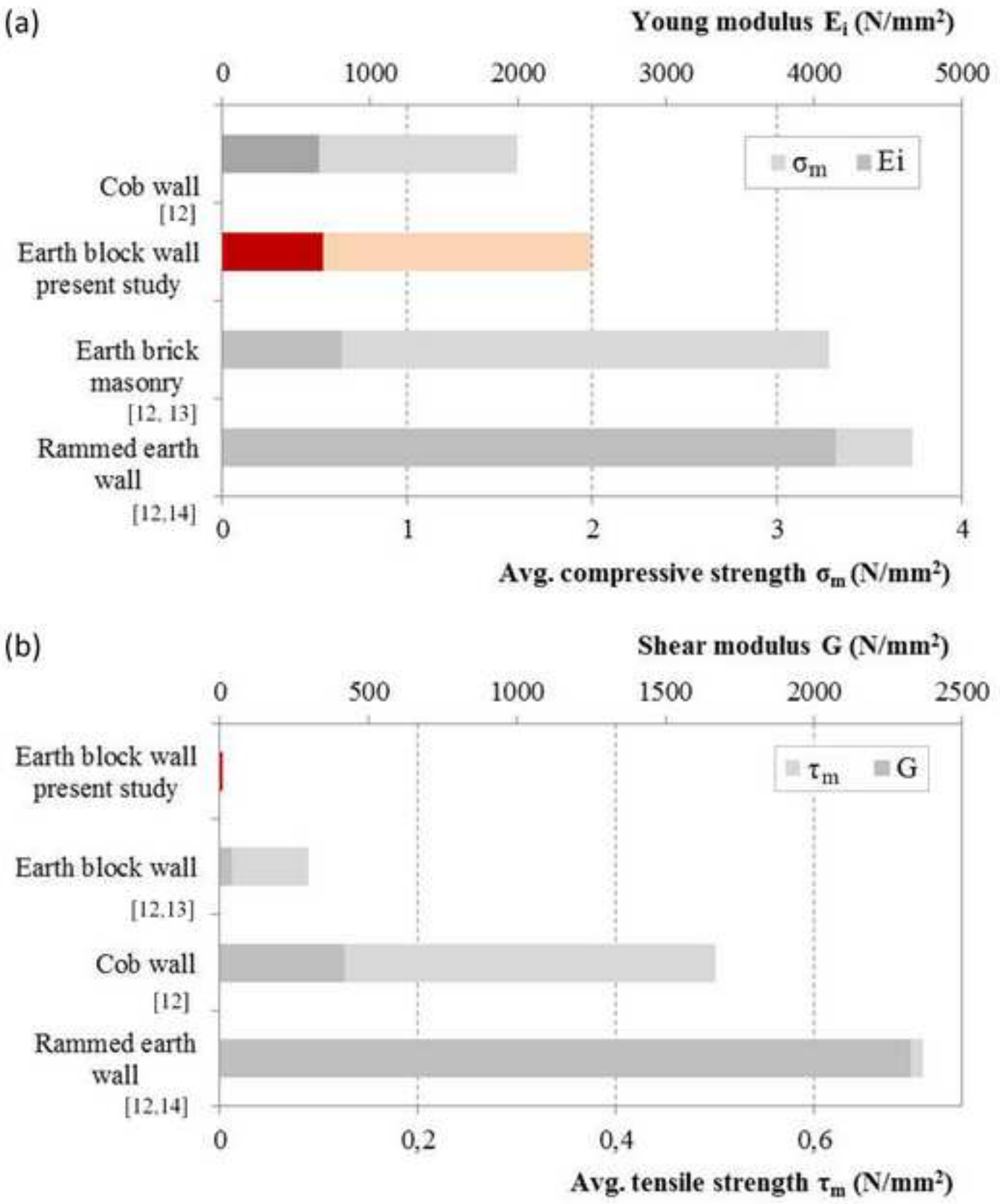

Figure 19

Click here to download high resolution image

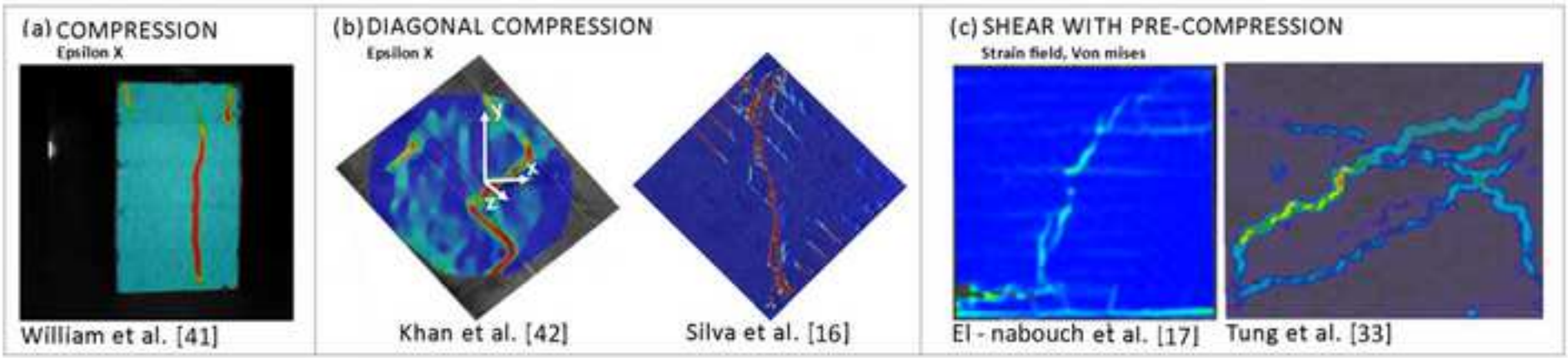

***Detailed Response to Reviewers**

The authors really thank the reviewers for their careful revision work and for the suggestions that allowed improving the paper.

Reviewer #1:

The manuscript presents an experimental study on the mechanical behaviour of a new earth block masonry. The new block developed is interesting, however, the content should be carefully revised at different points.

1. R: The title is not really convincing and give confusion, because DIC is just a technique which becomes now relatively popular. The author should decide what is the most important topic of the manuscript: "new earth block masonry" or DIC, to provide a relevant title.

A: The title has been changed in the following:

"Experimental study of the mechanical behaviour of a new extruded earth block masonry"

2. R: Section 2: "Main phase: characterization of the mechanical behavior of earth blocks wallettes through DIC technique to obtain the compressive and tensile strengths." However, the DIC technique helps to determine the displacements and then the strains, it does not enable to determine the compressive or tensile strength.

A: The text has been modified as follows:

"Main phase: characterization of the mechanical behavior of earth blocks wallettes through DIC technique to obtain the displacement and strain fields."

3. R: Section 2.1: the fibers used should be better described (size, ...). Section 2.1: a picture about the machine and the manufacturing process of the bricks should be added to provide a better understanding.

A: the authors have added a new text regarding the composition of the blocks and type of manufacturing process. The following text has been added in section 2.1. (Materials and sample preparation):

"Their composition consists of a matrix of clayey soil (70%) and spoils of rice husk fibers (30%) as natural stabilizers. The rice husk fibers have size of about 3 mm x 5 mm. The extruded blocks have been mechanically produced with the same manufacturing process used in brick factories, except for the oven and artificial drying chambers."

As regards the picture of the machine used for manufacturing process, the authors are not allowed from Ton-Gruppe Company to publish a detailed description of the extrusion tools, due to patent issues.

4. R: section 2.4: the authors should clarify the net compressive strength or gross compressive strength, how to determine those values. When the authors compare with the results from other studies, this point should be considered.

A: The author has clarified in the text that the net compressive strength has been considered (section 3). Moreover, in discussion section (section 7), we have specified that the comparisons with other solid and perforated blocks were possible since we have considered the net strength value.

5. R: Fig. 14: the accordance between DIC image and hand-draw is not convincing, while for Fig. 15 is more convincing.

A: To account for the reviewer observation we have adjusted the hand-drawn map through the photos taken during the experimental campaign.

If the author can revise carefully their manuscript, I think the manuscript can be considered for publication.

Reviewer #2:

The topic of the manuscript is interesting and can contribute to improve the knowledge on the mechanical behavior of earthen masonry. The manuscript is well written, methodology and significance are clearly described. To improve the overall quality of the manuscript, some minor revisions are suggested:

1. R: FIG 2 modify axis captions: percentage passing (%) - Sieve size (mm)

A: The figure was corrected as suggested.

2. R: FIG 3 Not relevant, the figure can be deleted.

A. Since the other reviewer required more details on blocks, such as fibres size, blocks extrusion method.., we find important to give information on blocks composition. So we have decided to replace the old figure with a new table (Table 3).

3. R: Section 7 In the framework of DIC comparison on earthen materials, it could be interesting to add the results on adobe masonry (Miccoli et al, 2015 Eng Struct) and rammed earth (Miccoli et al. 2015, Mater Struct).

A. The authors studied the works suggested by the reviewer and introduced the comparisons in the revised version in Section 7.

Highlights

- Mechanical properties of 12 masonry wallettes with earth blocks;
- Compression, diagonal compression and combined shear-compression tests;
- Digital image correlation (DIC) technique for data-processing;
- Crack maps and full-field strains maps.

***Declaration of Interest Statement**

Declaration of interests

☒ The authors declare that they have no known competing financial interests or personal relationships that could have appeared to influence the work reported in this paper.

☐The authors declare the following financial interests/personal relationships which may be considered as potential competing interests:

***Credit Author Statement**

Credit author statement

F. Stazi: Conceptualization, Investigation, Data Curation, Writing – Original Draft, Writing – Review & Editing
M. Serpilli: Conceptualization, Investigation, Data Curation, Writing – Original Draft, Writing – Review & Editing
G. Chiappini: Methodology & Software (DIC), Investigation, Data Curation (DIC)
M. Pergolini: Data Curation, Writing – Original Draft
E. Fratalocchi: Investigation, Data Curation (earthen material)
S. Lenci: Conceptualization, Supervision

*Title page

Experimental study of the mechanical behaviour of a new extruded earth block masonry

Francesca Stazi (a) **Corresponding author**
f.stazi@univpm.it.

Michele Serpilli (b)
m.serpilli@univpm.it.

Gianluca Chiappini(c)
g.chiappini@univpm.it

Marianna Pergolini (a)
m.pergolini@hotmail.it

Evelina Fratalocchi (a)
e.fratalocchi@univpm.it

Stefano Lenci (b)
s.lenci@univpm.it

(a) Department of Materials, Environmental Sciences and Urban Planning (SIMAU), Università Politcnica delle Marche, Italy.

(b) Department of Construction, Civil Engineering and Architecture (DICEA) Università Politcnica delle Marche, Italy.

(c) Department of Industrial Engineering and Mathematical Sciences (DIISM) Università Politcnica delle Marche, Italy.

Experimental study of the mechanical behaviour of a new extruded earth block masonry

Francesca Stazi[(a)]

Corresponding author

f.stazi@univpm.it

Michele Serpilli[(b)]

m.serpilli@univpm.it

Gianluca Chiappini[(c)]

g.chiappini@univpm.it

Marianna Pergolini[(a)]

m.pergolini@hotmail.it

Evelina Fratalocchi [(a)]

e.fratalocchi@univpm.it

Stefano Lenci [(b)]

s.lenci@univpm.it

(a) Department of Materials, Environmental Sciences and Urban Planning (SIMAU), Università Politcnica delle Marche, Italy.

(b) Department of Construction, Civil Engineering and Architecture (DICEA) Università Politcnica delle Marche, Italy.

(c) Department of Industrial Engineering and Mathematical Sciences (DIISM) Università Politcnica delle Marche, Italy.

Experimental study of the mechanical behaviour of a new extruded earth block masonry

F. Stazi[(a)], M. Serpilli[(b)], G. Chiappini[(c)], M. Pergolini[(a)], E. Fratalocchi[(a)], S. Lenci[(b)]

(a) Department of Materials, Environmental Sciences and Urban Planning (SIMAU), Università Politecnica delle Marche, Italy.

(b) Department of Civil and Construction Engineering, and Architecture (DICEA) Università Politecnica delle Marche, Italy.

(c) Department of Industrial Engineering and Mathematical Sciences (DIISM) Università Politecnica delle Marche, Italy.

Keywords: earth masonry; digital image correlation; shear behaviour; diagonal compression; failure mechanism; compressive behaviour; full-field strain.

ABSTRACT

The aim of this research is to investigate, through the Digital Image Correlation (DIC) technique, the mechanical performance of a new type of earth masonry, built with extruded blocks and characterized by dovetail horizontally staggered bed joints. The experimental program consists of two levels of investigations: (i) preliminary phase on components, (ii) compression, diagonal compression and combined shear-compression tests on 12 wallettes. Regarding the components, results showed that the mean compressive strength of the earth block was low (3.5 MPa) with respect to traditional bricks and similar to adobe blocks. The dovetail joints were effective in their joining role showing a rather good strength (2.4 MPa) when tested in triplet configuration. Regarding the wallettes, the DIC highlighted failure modes complying with the ones of a traditional masonry under shear, while it showed a "column behaviour" with vertical sliding under compressive tests. Fragile failures occurred during the diagonal compression test. DIC revealed to be a promising technique to recover the full-field strain and crack maps.

Nomenclature

f_c compressive strength of the earth block

f_{cm} average compressive strength of the earth block

f_{voi} initial shear strength

f_{vo} average initial shear strength

f_{vok} characteristic initial shear strength

E_i Young modulus

ν Poisson ratio

τ shear stress

σ normal stress

τ_m wall average shear strength

σ_m wall average compressive strength

G shear modulus

γ shear strain

ε normal strain

s_x horizontal displacement

s_y vertical displacement

1. Introduction

The present research focuses on a new type of masonry made of earth blocks. Benefits associated with the adoption of earth units include the improvement of the building energy efficiency [1, 2], and its environmental and economic sustainability [3-5]. The blocks are made of a mixture of natural components, namely clay, water and rice husk fibres. Clay acts as a natural binder and confers strength to the blocks but it can be subject to cracks due to drying shrinkage [6]. This drawback can be reduced through the addition of stabilizers. Numerous studies suggest the use of both natural [7-9] and artificial [10] fibres to prevent the outbreak of tensile forces and the consequent drying shrinkage [11]. Another relevant feature affecting the performance of earth blocks is represented by the manufacturing process that can vary from manual to fully automated [12-14]. The extrusion of bricks is a promising method, determining strengths comparable with those of traditional fired bricks [15].

While there is a lot of literature on mechanical behavior of stone and fired brick masonries, the knowledge on extruded earth blocks constructions is very limited. Indeed the literature on earthen wallettes mainly regards the most commonly used earth construction techniques, namely rammed earth [12, 14, 16 and 17] and cob [12], while the studies on extruded earth block masonries are very rare. The earth blocks adopted in [12] and [13] are brick-like units produced by a mechanized hand-moulding procedure, horizontally layered with mortar bed joints, thus recreating a traditional masonry wall.

In this research, we have selected extruded perforated blocks with rice husk, to couple a natural stabilization method with the most advantageous manufacturing technique (Fig.1a). The block is novel since the extrusion is uncommonly-realized at industrial scale, providing a major structural potential with respect to usual blocks, which are manually or mechanically compressed within a mold. Moreover, a novel assembly technique for the masonry construction is adopted, providing horizontally staggered bed joints (thus creating aligned vertical joints), linked through tongue and groove dovetail connections. This technique is at the present used in both exterior and interior sides of timber framed constructions (Fig.1 b and c), fixed by means of ring-shank nails to the external bracing fir boards, with energy saving and shear-collaborating issues, but without load bearing functions.

In the present work, the new earth block masonry was surveyed through Digital Image Correlation (DIC). In recent years, this technique has become one of the most promising measurement methods, since it allows obtaining a significant amount of information on the strain state of the material/structure and a complete reconstruction of the crack pattern [18]. Several authors have

advantageously applied DIC in different frameworks, such as the analysis of the mechanical behaviour of reinforced concrete beams [19-21], composites [20] and masonry.
Its application on masonries was carried out at different scales: characterization of small specimens of reinforcing mortars [21]; investigation of the bonding behaviour in FRP–brick specimens interfaces [22]; survey of the mechanical behaviour of small-scale masonry units [23]; tests on wallettes and full-scale prototypes ([24] and [25]); mechanical study of real-scale confined masonry walls [26]; map of the crack propagation at the building scale [27].

The present research is aimed at characterizing the mechanical properties of a new type of masonry with horizontally staggered bed joints, made of extruded earth blocks by means of the DIC technique and evaluating possible applications of such blocks for load bearing functions.
To that aim, an extensive experimental campaign has been carried out by means of compression and shear tests on small samples and wallettes. All measurements have been recorded with the aid of DIC technique and processed via MatLab.

2. Test methods

The research phases are the following:

- Preliminary phase: material characterization of earth blocks to obtain the compressive strength of single units and the initial shear strength of triplets.
- Main phase: characterization of the mechanical behavior of earth blocks wallettes through DIC technique to obtain the displacement and strain fields.

A detailed outline of the lab tests of the main phase is summarized in Table 1.

2.1. Materials and samples preparation

The hollow extruded earth blocks were provided by Ton-Gruppe Construction Company.
Their composition consists of a matrix of clayey soil (70%) and spoils of rice husk fibers (30%) as natural stabilizers. The rice husk fibers have size of about 3 mm x 5 mm. The extruded blocks have been mechanically produced with the same manufacturing process used in brick factories, except for the oven and artificial drying chambers.
The soil matrix was tested to determine its grain size distribution (ASTM D422) and consistency limits (ASTM D4318). All the soil passed the #200 sieve (opening 0,075 mm) and resulted a lean clay according to the Unified Soil Classification System, USCS (ASTM D2487), as shown in Table

2 and Fig. 2. The activity coefficient, equal to about 1, reveals a normally active soil, with a low susceptibility to swelling or shrinkage. X-ray diffractometry revealed that the main mineralogical components are calcite, montmorillonite and gypsum as shown in Table 3.

The tested samples consisted of 9 single blocks, 6 triplets and 12 wallettes.

The block is extruded through a die machine and left naturally air-dried. Each earth unit has nominal dimensions of (215 x 230 x 115 mm^3) and presents one flat vertical surface and one ribbed side to improve the adhesion of the external plaster **(**Fig. 1a**)**. On the lateral surfaces, dovetail joints serve as a guide for the alignment of the earth units during the wall assembly and ensure their mechanical connection, thus enhancing the overall global behavior. A novel technique for the wall assembly with horizontally staggered bed joints is adopted. Thus, the blocks are aligned along vertical columns and are linked together through the aforementioned dovetail joints.

The wallets size was 1.07 x 1.03 x 0.11 m^3. Their realization comprised the following steps: (i) clay was mixed with water in a ratio of 2:1; (ii) the lateral and the bottom surfaces of each block were uniformly wetted in this paste; (iii) each block was then secured to the others by vertically sliding it along their dovetail joints.

Preliminary tests on mortar samples (UNI EN 1015-11:2017) revealed values of 0.21 N/mm^2 and 1.83 N/mm^2, respectively for flexural and compression strengths. The upper bed of each specimen was leveled to remove excess material as to guarantee a plane surface for the subsequent load application.

All materials and assemblies were stored in the laboratory until testing and the curing process lasted 30 days in a controlled laboratory environment.

2.2. Preliminary tests on the earth blocks

The net compressive strength of nine uncapped earth blocks (Fig. 3a) was determined in accordance to the UNI EN 772-1:2015 standard. The testing apparatus was a hydraulic press machine (maximum load capacity of 5000 kN). The rate of compression was set at 0.05 ($N/mm^2/s$). The earth blocks were tested in the extrusion direction.

The initial shear strength parallel to the dovetail joints (Fig. 3b) was determined on 3 specimens according to UNI EN 1052-3:2007 standard (Procedure B). The test set up involved the use of two 20-mm thick plates at the top and at the bottom of the specimen. Compressive load was applied on the top plate using of Zwick Roell Z050 testing machine (maximum load of 1000 kN) in force control at a rate of 2645 N/min until failure.

The initial shear strength perpendicular to the dovetail joints (Fig. 3c), subject to an out-of-plane load, was evaluated on 3 specimens by adopting the same UNI EN 1052-3:2007 standard procedure.

2.3. DIC Set-up

The displacement and deformation of the surface of the wallettes were measured using the 3D-DIC technique. The region of interest (ROI) on each side of the wallettes has been spray-painted with black and white texture. Preliminary tests were carried out to define the most suitable dimensions and intensity of the pattern, following [24]. The experimental set-up is presented in Fig. 4. The features of the two cameras (model Pixelink® B371F – see insert A in Fig. 4) and the calibration data are shown in Table 4.

A third camera (insert A in Fig. 4) was used to check, with DIC-2D, the displacement and the deformation of the backside. During the tests, the manometer was coupled with an additional high-resolution camera that acquired the frames needed to register the pressure trend against time. Then, compression and tensile strengths values were obtained, according to the relative test standards.

The pictures of the wallettes acquired during the tests have been post-processed by a 3D-DIC software. The correlation method between the two cameras and the deformed images was based on global DIC, which incorporates the epipolar constraint and the assembling approach of Finite Element method. The displacements of all grid measuring points, created on the entire surface of the wallettes, were obtained by minimizing the correlation error computed all over the current frame with respect to the reference frame [25]. The zero-mean sum of square difference (ZSSD) criterion has been adopted to avoid the effects of lighting offset and inhomogeneity.

Fig. 5a presents one of the pictures recorded by the frontal camera with the overlaid measurement grid. The subsets discretization, used for the DIC analysis, was 25×25 pixels meaning each measure point was about 20 mm. Fig. 5b shows the 3D grid calculated by the stereo triangulation with the schematic position of the two frontal cameras. The strains (γ_x, γ_y, and γ_{xy}) have been computed by means of the Cauchy-Green theory, starting from the 3D node displacements. Several authors have already successfully applied this method on tests of different materials: metals, ceramic, foam, cork and FRCM [28-32].

In a preliminary phase, the quality of the correlation technique and strains measurements was assessed through a set of 50 stationary images. Fig. 5c illustrates the average values of the vertical strain distribution (ε_y) and its standard deviation within each frame. The average strain presents small random oscillations around zero and the standard deviations are nearly constant, in the order

of 100 με. The crack maps were obtained by calculating the equivalent Von Mises strain in plane strain conditions (γ_3=0) [33].

$$\varepsilon_{VM} = \sqrt{\frac{2\left[(\varepsilon_1 - \varepsilon_2)^2 + \varepsilon_1^2 + \varepsilon_2^2\right]}{3}} \quad (1)$$

To avoid visualizing the sliding effect between columns of bricks, the crack maps were calculated by creating measurement grids on each brick column separately.

2.4. Tests on the wallettes

The compressive strength of the wallettes (Fig. 6a) was determined on 3 samples according to UNI EN 1052-1. The specimens were subject to a compression load by means of two 500 kN hydraulic jacks, uniformly distributed thanks to a 25 mm-thick steel plate. The nominal strains ε were obtained by averaging the strain values recorded through DIC on the whole specimen area.

The shear strength of the wallettes (Fig. 6b) was obtained through diagonal compression tests on 3 samples following the ASTM E519 – 07 standards. The shear test apparatus consisted of a single hydraulic jack (500 kN). The shear strain γ was estimated through DIC, as the mean value of the γ recorded on the ROI.

The shear strength of the wallettes under a constant pre-compression load (Fig. 6c) was obtained on 3 samples following the experimental guidelines provided by [34], using a pre-compression load of 0.2 N/mm^2. An "L" shaped steel profile was placed on the upper part of the specimen to transmit the horizontal force.

3. Results of preliminary tests

The compressive strengths of the earth blocks, referred to the net area (the area of the surface on which the load is applied excluding the voids), are summarized in Table 5.

The average net compressive strength f_{cm} was found to be 3.4 N/mm^2. As expected, this value is quite low as compared to the compressive strength of traditional solid baked bricks, commonly around 16 N/mm^2 [35].

The failure mode was the same for all the specimens tested, with cracks originating before the peak load (Fig. 7a). Cracks were located on the front and backsides of the blocks, close to the point of application of the load.

The average and characteristic initial shear strengths f_{voi} and f_{vok} parallel and perpendicular to the dovetail joints are reported in Table 6. The characteristic initial shear strength f_{vok} parallel to the dovetail joints was 0.03 N/mm^2. The coefficient of variation (COV) is relatively high, as typical in handmade assembled constructions. The typical failure mode is reported in Fig. 7b. The characteristic initial shear strength f_{vok} perpendicular to the dovetail joints was 1.90 N/mm^2. The failure mode is reported in Fig. 7c, denoting a good interlocking effect of the dovetail joint and corner expulsion.

4. Normal Compression tests

4.1 Stress-strain curves

The stress – strain σ - ε diagrams for the 3 wallettes are shown in Fig. 8, where the strain values were obtained through DIC and post-processed in MATLAB. The specimens exhibited an approximately linear behaviour up to the maximum load with a brittle failure.

The mean value σ_m, Young's modulus determined at 1/3 of maximum stress E_i and Poisson's ratio ν of the wallettes are summarized in Table 7. The mean value of σ_m was approximately 2 N/mm^2.

4.2 Full field strain maps

The DIC allowed recovering the complete deformation field at each point of the wall. The evolution in time of the vertical displacement s_y, the vertical strain ε_y and the shear strain γ_{xy}, are shown in three distinct frames (Fig. 9) corresponding to the three highlighted points of Fig. 8.

From the evolution of s_y it could be noted that the wall behaves as a series of independent slender adjacent columns (Fig. 9a). Indeed, the alignment of the vertical joints avoids the uniform downward distribution of the load. This behavior leads to a modest out-of-plane instability phenomenon (confirmed by the 3D-DIC), which is mitigated by the presence of the dovetail joints. The "column effect" is also visible by the evolution of the γ_{xy} that registered high relative sliding between the vertical members (Fig. 9b). As expected, the ε_y is uniformly distributed on the ROI surface with some evident areas of strain concentration (Fig. 9c).

4.3 Full field cracks map

The cracks map under uniaxial compression load obtained through a visual survey is compared with the Von Mises strain map obtained by DIC, in Fig. 10. The cracks propagated from the upper region of the specimens along the masonry surface, with clay expulsions in proximity of the applied force.

The DIC results confirm those obtained by visual inspection and highlight more in detail the weak points. Some vertical cracks, not referable to typical tensile block failures, are located in the proximity of the wall top edge due to an expulsion mechanism.

5. Diagonal compression tests

5.1 Stress-strain curves

The shear stress–strain $\tau - \gamma$ curves for the 3 wallettes are presented in Fig. 11. It can be noted a distinctive yield point when elasticity of the specimen is exceeded and first cracks appeared. The tensile strength τ_m, shear modulus G and shear strain γ of the wallettes are reported in Table 8. The diagonal compression test registered a very low average strength value τ_m (0.002 N/mm^2). This value is due to the specific construction technique which relies only on the friction between the horizontal and the vertical dovetail joints since the thin mortar layer is characterized by low resistance.

5.2 Full field strain maps

The evolution in time of s_x, s_y and γ_{xy}, is illustrated for three distinct moments (see Fig. 12) corresponding to the three highlighted points of Fig. 11. The s_x and s_y maps show that the specimen open up in two parts laterally facing the loading line. This behavior is due to the low adhesion at the interface between the blocks (Fig.12a, b). Additionally, sliding along the joint lines was also visible from the γ_{xy} maps (Fig.12c).

5.3 Full field cracks map

The cracks map under a diagonal compression load derived from a visual inspection is presented in Fig. 13 and is compared with the Von Mises strain map obtained by DIC. All the specimens exhibited a brittle behavior. Fragile-type cracks originated very close to the normal loading line and propagated through the joints, without damaging the blocks. At the end of the tests, all the wallettes were completely disrupted. The DIC successfully reproduced the visual inspection, giving adjunctive information on the strain field.

6. Shear tests with pre-compression

6.1 Stress-strain curves

The results of the shear stress–strain τ-γ diagrams for the 3 specimens subject to a pre-compression load of 0.2 N/mm^2 are presented in Fig. 14. In the first part, the curves showed a linear trend until the first crack appeared. Then, a plastic region occurred with formation of other diagonal cracks. The trend showed a ductile behaviour, typical of shear tests with pre-compression. The tensile strength τ_m, shear modulus G and shear strain γ of the wallettes are collected in Table 9. As expected, the test showed a slight increase (about 2.4%) in terms of tensile strength with respect to the diagonal tensile findings without pre-compression.

6.2 Full field strain maps

The evolution in time of s_x, s_y and γ_{xy} for the wallettes under shear combined with pre-compression are shown in Fig. 16. As expected, the displacement s_x presented an approximately linear trend along the vertical axis (Fig. 15a). The displacement s_y showed a relevant sliding along the vertical joints. This phenomenon has already been pointed out in the full strain maps of the compression test (Fig. 15b). In the strain γ_{xy} maps, two inclined crack lines originating from the point of application of the shear force were visible (Fig. 15c).

6.3 Full field cracks map

The hand-drawn cracks map of the specimens under shear and constant compression load is compared with the Von Mises strain map in Fig. 16. As expected, the failure mechanism highlights diagonal staggered fractures following the vertical and horizontal lines of the joints.

7. Discussion

The present research experimentally investigated through DIC the mechanical behaviour of a new earth block masonry, characterized by industrially extruded units assembled in vertical columns, connected by dovetail joints, and with staggered horizontal bed joints. In particular, the objective was to verify the shear performance and the possible load bearing functions.

The data have proved that the masonry units have low compressive strength, typical of earthen blocks. The average net compressive strength σ_m of the single unit (earth block with dovetail joints) was compared in Fig. 17a with the ones of either unbaked bricks with different mixtures.

The f_{cm} values of the present perforated blocks can be compared with the values obtained in literature regarding experimentations on solid blocks, since the net compressive strength excludes the voids influence. The net strength values are similar to those of solid blocks, namely adobe

bricks [36] earth blocks with coarse sand [37] and manually compressed earthen blocks [37], while they are much lower than those achieved by perforated earth blocks with mechanical compression manufacturing techniques [38].

The average tensile strength τ_m parallel to the dovetail joints of the triplet was compared with the ones of several triplet configurations made of different brick and mortar assemblies [39, 40] (Fig. 17b). The low value of the tensile strength of the present technique is comparable with that of other techniques characterized by poor quality mortar.

The values of the average compressive strength σ_m and the Young modulus E_i of the wallettes were compared with the ones of other earth walls (Fig. 18a). The σ_m and E_i values obtained in the present study (1.59 N/mm^2 and 651 N/mm^2, respectively) were comparable with those of the cob wall but significantly lower than the ones of the rammed earth and earth block walls [12-14]. The low compressive strength of the experimented earth wallette is due to: (i) the particular block adopted here, that is perforated, differently by other studies (e.g. [12 and 13]) that surveyed solid block configurations; (ii) the particular assembly technique, which does not provide the uniform downward load distribution.

The tensile strenght τ_m and shear modulus G of the earth wallette, obtained with diagonal compression tests, were compared with the results of the same aforementioned earth masonries in [12-14] (Fig. 18b). As already mentioned, the earth wallette under study, exhibited a scarce shear behaviour. Indeed, the values of tensile strength (0.002 N/mm^2) and shear modulus (8.68 N/mm^2), were the lowest.

The findings were compared with the experimental results by other authors in literature regarding other masonry samples surveyed through DIC (Fig. 19).

The DIC applied on compression tests (see Fig. 10 and Fig. 19a) revealed the absence of tensile block failure characterized by vertical cracks through the blocks that typically occurs under compression in traditional brick masonries (e.g. [41]) and earthen block masonries with horizontal courses (e.g. [13]). This behaviour is due to the lack in the present wall of a deformable mortar layer, which causes horizontal tensions within the blocks. Moreover, the crack pattern in the present work reveals also a different failure behaviour respect to the one observed in rammed earth wallettes (see e.g. [14]), characterized by the formation of cone shaped cracks at the upper and lower regions.

The DIC on diagonal compression tests showed the presence of weak planes along the bed joints, as also highlighted by other authors regardless the block material and size (see Fig. 13 and Fig. 19b).

For concrete masonry, the strain accumulation was located along the mortar joints where failure occurred [42]. Also for rammed earth, the DIC allowed to visualizing the fracture lines along the compaction layers [16].

The DIC on shear tests with pre-compression highlighted the formation of cracks along the diagonal compressive strut following the staggered lines of the bed joints (see Fig. 16). The shear tests was also evaluated through DIC in [17], [33] and [43]. The former study found quasi-diagonal cracks in rammed earth walls, while the latter two observed more sharply diagonal cracks for traditional fired clay and concrete masonry, respectively (Fig. 19c).

The results clearly showed the capability of DIC to identify the regions with strains concentrations and therefore to locate the position of eventual failure mechanisms.

8. Conclusion

In this paper, the mechanical properties of a new type of earth blocks masonry have been investigated by means of DIC.

The study of the mechanical behavior of the single block and of the joints gave the following results:

- Compressive strength of the earth block was low (3.5 MPa), but comparable with the values of adobe blocks;
- The tensile strength, evaluated in triplets, was low (0.04 MPa) regardless the presence of the dovetail joints.

The study of the mechanical behavior of 12 wallettes under compression, shear and a combination of them, gave the following results:

- The compression tests highlighted that the geometry of the block coupled with the horizontally staggered wall assembly led to a “column behavior” differently from traditional masonries. During the test, a differential sliding between bricks columns occurred;
- The diagonal compression tests registered a low tensile resistance value since the low quality earth mortar coupled with the joints vertical alignment did not guarantee a proper bond between the blocks thus enhancing the fragile behavior and the assembly disruption.
- The shear tests under pre-compression loads showed the formation of compressive struts typical of masonries and revealed a slight increase in terms of tensile strength with respect to the diagonal tensile findings without pre-compression, due to the collaboration of the dovetail joints.

In general, the study showed the need to improve the mechanical properties of the earth blocks and the connection ability of the dovetail joints to achieve possible bracing capacities of the walls made

with this technology. The DIC technique was successfully implemented to determine the deformation and failure state of the earth blocks masonries. The full-field measurements using DIC technique is promising, especially when the specimens are subject to inelastic deformations. Moreover, the DIC proved its high potential in stress-strain monitoring.

Acknowledgements

The authors thank TON-GRUPPE ® for having provided the material and particularly Eng. Marco Tinti for his support on the wallettes manufacturing.

REFERENCES

REFERENCES

[1] D. Allinson and M. Hall, "Hygrothermal analysis of a stabilised rammed earth test building in the UK," Energy Build., vol. 42, no. 6, pp. 845–852, 2010.

[2] P. Taylor and M. B. Luther, "Evaluating rammed earth walls : a case study," Sol. En., vol. 76, pp. 79–84, 2004.

[3] F. Pacheco-Torgal and S. Jalali, "Earth construction: Lessons from the past for future eco-efficient construction," Constr. Build. Mater., vol. 29, pp. 512–519, 2012.

[4] B. V. Venkatarama Reddy and P. Prasanna Kumar, "Embodied energy in cement stabilised rammed earth walls," Energy Build., vol. 42, no. 3, pp. 380–385, 2010.

[5] O. Bayode, Y. Michael, and D. Adedeji, "Review of economic and environmental bene fi ts of earthen materials for housing in Africa," Front. Archit. Res., vol. 6, no. 4, pp. 519–528, 2017.

[6] E. Quagliarini and S. Lenci, "The influence of natural stabilizers and natural fibres on the mechanical properties of ancient Roman adobe bricks," J. Cult. Herit., vol. 11, no. 3, pp. 309–314, 2010.

[7] V. Sharma, B. M. Marwaha, and H. K. Vinayak, "Enhancing durability of adobe by natural reinforcement for propagating sustainable mud housing," Int. J. Sustain. Built Environ., vol.

5, no. 1, pp. 141–155, 2016.

[8] K. Ghavami, D. T. Filho, and N. P. Barbosac, “Cement & Concrete Composites Behaviour of composite soil reinforced with natural fibres,” Cement and concrete composites, vol. 21, pp. 39–48, 1999.

[9] Ş. Yetgin, Ö. Çavdar, and A. Çavdar, “The effects of the fiber contents on the mechanic properties of the adobes,” Constr. Build. Mater., vol. 22, no. 3, pp. 222–227, 2008.

[10] H. Binici, O. Aksogan, and T. Shah “Investigation of fibre reinforced mud brick as a building material,” Constr. Build. Mat., vol. 19, pp. 313–318, 2005.

[11] C. H. Kouakou and J. C. Morel, “Applied Clay Science Strength and elasto-plastic properties of non-industrial building materials manufactured with clay as a natural binder,” Appl. Clay Sci., vol. 44, no. 1–2, pp. 27–34, 2009.

[12] L. Miccoli, U. Müller, and P. Fontana, “Mechanical behaviour of earthen materials: A comparison between earth block masonry, rammed earth and cob,” Constr. Build. Mater., vol. 61, pp. 327–339, 2014.

[13] L. Miccoli, A. Garofano, P. Fontana, and U. Müller, “Experimental testing and finite element modelling of earth block masonry,” Eng. Struct., vol. 104, pp. 80–94, 2015.

[14] L. Miccoli, D. V. Oliveira, R. A. Silva, U. Müller, and L. Schueremans, “Static behaviour of rammed earth: experimental testing and finite element modelling,” Mater. Struct. Constr., 2015.

[15] D. Maskell, A. Heath, and P. Walker, “Laboratory scale testing of extruded earth masonry units,” J. Mater., vol. 45, pp. 359–364, 2013.

[16] R. A. Silva, O. Domínguez-martínez, D. V Oliveira, and E. B. Pereira, “Comparison of the performance of hydraulic lime-and clay-based grouts in the repair of rammed earth,” Constr. Build. Mater., vol. 193, pp. 384–394, 2018.

[17] R. El-nabouch, Q. Bui, O. Plé, and P. Perrotin, “Assessing the in-plane seismic performance of rammed earth walls by using horizontal loading tests,” Eng. Struct., vol. 145, pp. 153–161, 2017.

[18] N. McCormick and J. Lord, “Digital image correlation,” Mater. Today, vol. 13, no. 12, pp. 52–54, 2010.

[19] M. Di Benedetti, S. Cholostiakow, H. Fergani, E. Zappa, A. Cigada, and M. Guadagnini "3D-DIC for strain measurement in small scal GFRP RC specimens", Proceedings of SMAR 2015, 3rd conference on smart monitoring, Antalaya, Turkey .

[20] M. Tekieli, S. De Santis, G. de Felice, A. Kwiecień, and F. Roscini, "Application of Digital Image Correlation to composite reinforcements testing," Compos. Struct., vol. 160, pp. 670–688, 2017.

[21] C. Caggegi, D. Sciuto, and M. Cuomo, "Experimental study on effective bond length of basalt textile reinforced mortar strengthening system: Contributions of digital image correlation," Meas. J. Int. Meas. Confed., vol. 129, no. June, pp. 119–127, 2018.

[22] B. Ghiassi, J. Xavier, D. V Oliveira, A. Kwiecien, and P. B. Lourenço, "Evaluation of the bond performance in FRP – brick components re-bonded after initial delamination," Compos. Struct., vol. 123, pp. 271–281, 2015.

[23] D. Markulak, T. Dokšanović, I. Radić, and I. Miličević, "Structurally and environmentally favorable masonry units for infilled frames," Eng. Struct., vol. 175, no. March, pp. 753–764, 2018.

[24] M. A. Sutton, F. Matta, D. Rizos, R. Ghorbani, S. Rajan, and D. H. Mollenhauer, "Recent Progress in Digital Image Correlation : Background and Developments since the 2013 W M Murray Lecture," Exp. Mech., pp. 1–30, 2017.

[25] N. Guerrero, M. Martinez, R. Picòn, M.E. Marante, F. Hild, and S. Roux, "Experimental analysis of masonry infilled frames using digital image correlation," Mater. Struct., vol. 47, no. 5, pp. 873–884, 2014.

[26] R. Ghorbani, F. Matta, and M. A. Sutton, "Full-Field Deformation Measurement and Crack Mapping on Confined Masonry Walls Using Digital Image Correlation," Exp. Mech., vol. 55, no. 1, pp. 227–243, 2015.

[27] E. Speranzini, R. Marsili, M. Moretti, and G. Rossi, "Image Analysis Technique for Material Behavior Evaluation in Civil Structures," Materials (Basel)., vol. 10, no. 7, p. 770, 2017.

[28] D. Amodio, G. B. Broggiato, E. Campana, and G. M. Newaz, "Digital Speckle Correlation for Strain Measurement by Image Analysis," Exp. Mech., vol. 43, no. 4, pp. 396–402, 2003.

[29] G. Chiappini, M. Sasso, T. Bellezze, and D. Amodio "Thermo-structural analysis of components in ceramic material," Procedia Struct. Integr., vol. 8, pp. 618–627, 2018.

[30] F. Stazi, F. Tittarelli, F. Saltarelli, G. Chiappini, A. Morini, G. Cerri, and S. Lenci, "Carbon nano fibers in polyurethane foams : Experimental evaluation of thermo-hygrometric and mechanical performance," Pol. Test., vol. 67, no. September 2017, pp. 234–245, 2018.

[31] M. Sasso, E. Mancini, G. Chiappini, F. Sarasini and J. Tirillò "Application of DIC to Static and Dynamic Testing of Agglomerated Cork Material," Exp. Mech., pp. 1017–1033, 2018.

[32] J. Donnini, G. Chiappini, G. Lancioni, and V. Corinaldesi, "Tensile behaviour of glass FRCM systems with fabrics' overlap : Experimental results and numerical modeling," Compos. Struct., vol. 212, no. January, pp. 398–411, 2019.

[33] S. Tung and M. Shih, "Development of digital image correlation method to analyse crack variations of masonry wall," vol. 33, no. December, pp. 767–779, 2008.

[34] E. Quagliarini, S. Lenci, and M. Iorio, "Mechanical properties of adobe walls in a Roman Republican domus at Suasa," J. Cult. Herit., vol. 11, no. 2, pp. 130–137, 2010.

[35] H. U. Sajid, M. Ashraf, Q. Ali, and S. H. Sajid, "Effects of vertical stresses and flanges on seismic behavior of unreinforced brick masonry," Eng. Struct., vol. 155, no. April 2017, pp. 394–409, 2018.

[36] R. Illampas, I. Ioannou, and D. C. Charmpis, "Adobe bricks under compression : Experimental investigation and derivation of stress – strain equation," Constr. Build. Mater., vol. 53, pp. 83–90, 2014.

[37] Q. Piattoni, E. Quagliarini, and S. Lenci, "Experimental analysis and modelling of the mechanical behaviour of earthen bricks," Constr. Build. Mater., vol. 25, no. 4, pp. 2067–2075, 2011.

[38] J. D. Sitton, Y. Zeinali, W. H. Heidarian, and B. A. Story, "Effect of mix design on compressed earth block strength," Constr. Build. Mater., vol. 158, pp. 124–131, 2018.

[39] V. Alecci, M. Fagone, T. Rotunno, and M. De Stefano, "Shear strength of brick masonry walls assembled with different types of mortar," Constr. Build. Mater., vol. 40, pp. 1038–1045, 2013.

[40] V. Corinaldesi and G. Moriconi, "Behaviour of cementitious mortars containing different kinds of recycled aggregate," Constr. Build. Mater., vol. 23, no. 1, pp. 289–294, 2009.

[41] K. Willam, A. Mohammadipour, R. Mousavi, and A. S. Ayoub, "Failure of Unreinforced Masonry Under Compression," Structures congress 2013, pp. 2949–2961, 2013.

[42] F. Khan, A. Kontsos, I. Bartoli, and M. Bolhassani, "Using DIC to measure deformation fields of concrete masonry test specimens," 12th Canadian Masonry Symposium, June, 2013.

[43] F. Khan, R. Carmi, S. Rajaram, and M. Bolhassani, "Multiple cross validated sensing system for damage monitoring in civil structural components" Proceedings of the 9 th International Workshop on Structural Health Monitoring 2013, January, 2013.

List of captions

Fig. 1. (a) Earth block geometry, (b) Platform-Frame construction system and (c)external envelope layers.

Fig. 2. Grain size distribution of the soil matrix.

Fig. 3. Tests set up for (a) the determination of the compressive strength of the earth block, (b) the determination of the initial shear strength parallel to the dovetail joints (configuration A) and (c) the determination of the initial shear strength perpendicular to the dovetail joints (configuration B).

Fig. 4. DIC set up.

Fig. 5. (a) Picture whit overlaid grid, (b) 3D grid point, and (c) strain noise evaluation for the 3D-DIC.

Fig. 6. Tests set up of the wallette specimen for (a) the determination of its compressive strength, (b) the determination of its tensile strength and (c) the determination of its shear strength with a constant compression load.

Fig. 7. Failure modes of (a) the earth block, (b) of the triplet (configuration A) and (c) of the triplet (configuration B).

Fig. 8. $\sigma - \varepsilon$ curves of the wallette specimens under compression load.

Fig. 9. Complete displacement and strains fields of the wallettes under compression load.

Fig. 10. Crack mapping on wallette under compression load: (a) Von Mises strain field of the ultimate state and (b) hand-drawn map based on visual inspection.

Fig. 11. τ-γ curves of the wallette specimens under diagonal compression load.

Fig. 12. Complete displacements and strain fields of the wallettes under diagonal compression load.

Fig. 13. Crack mapping on wallette diagonal compression load: (a) Von Mises strain field of the ultimate state and (b) hand-drawn map based on visual inspection.

Fig. 14. τ-γ curves of the wallette specimen under a shear and constant compression of 0.2 N/(mm^2).

Fig. 15. Complete displacements and strain fields of the wallettes under a shear and constant compression of 0.2 N/(mm^2).

Fig. 16. Crack mapping on wallette under shear and pre-compression load: (a) Von Mises strain field of the ultimate state and (b) hand-drawn map based on visual inspection.

Fig. 17. Comparison of (a) the compressive strength values of different types of bricks and (b) of the initial shear strength of triplet setups.

Fig. 18. Comparison of (a) the compressive strengths, and (b) the tensile strengths of different types of masonries obtained from a diagonal compression load.

Fig. 19. Results of the DIC technique applied in masonries under (a) compression load, (b) diagonal compression load and (c) shear with pre-compression.